Mascle, J., Lohmann, G.P., and Moullade, M. (Eds.), 1998
Proceedings of the Ocean Drilling Program, Scientific Results, Vol. 159

43. INDICATORS OF CLIMATE AND SEDIMENT-SOURCE VARIATIONS AT SITE 959: IMPLICATIONS FOR THE RECONSTRUCTION OF PALEOENVIRONMENTS IN THE GULF OF GUINEA THROUGH PLEISTOCENE TIMES[1]

P. Giresse,[2] F. Gadel,[2] L. Serve,[3] and J.P. Barusseau[2]

ABSTRACT

Leg 159 Ocean Drilling Project Site 959 (in 2100 m water depth and ~120 km off the west African coast) is located on a small plateau that extends on the northern flank of the Côte d'Ivoire-Ghana Marginal Ridge. Because of its topographic position, this site was largely isolated from mass gravitational or turbidity flows coming from the continental shelf and slope. This very steep transform margin, on the other hand, has probably established interference of bottom-water circulation. The Hole 959C depth corresponds roughly to the interface between North Atlantic Deep Water and South Atlantic Intermediate Water. The very moderate linear sedimentation rates (~1–2 cm/k.y.) are relatively constant throughout the Pleistocene interval. This pronounced low sedimentation rate most likely reflects the persistent activity of deep-water circulation. Based on the oxygen isotopic record, two stratigraphic gaps are reported between 1.6 and 0.99 Ma and between 0.20 and 0.12 Ma, and are attributed to enhanced bottom-water circulation. This water circulation implies that significant changes in winnowing activity occurred in this site during the last 1 m.y. Detailed microstructural analysis indicates a number of laminae 1 mm to 1 cm thick with increased concentration of foraminifers resulting from the recurrent winnowing process (contourite). Many more glauconitic infillings of foraminifers were observed ~1–0.9 Ma, just after the major hiatus. Assuming that the superficial redistribution of the sediment was favorable to longer contact with seawater and to mineralization, the green grain concentration supports the indication of an uneven beginning of sedimentation after the hiatus.

The carbonate average concentrations tend to increase from ~20%–30% in the lower part of the section to ~35%–40% in the upper part. Organic carbon increases ~0.7%–0.8% in the lower part to 1%–1.1% in the upper part. However, accumulation rates for carbonate and organic carbon closely follow bulk accumulation rate records that correspond to an average of the bottom-current winnowing intensity. Consequently, cyclic variations in relative abundances of carbonate and noncarbonate components do not appear to correspond clearly or closely to glacial/interglacial cycles. The older section (before 1.5 Ma) shows some evidence of maxima in productivity of calcareous foraminifers during interglacial cycles. Conversely, maxima of organic carbon are connected to glacials and may be enhanced by local upwelling. Both of these indicators have been used in the same way to identify the steps of the last 125 k.y. Such cyclic variations are similar to those of neighboring sites on the slope of the eastern equatorial Atlantic, but from ~1 to ~0.2 Ma, the highest variabilities are recorded and attributed to enhanced sediment redistribution. In the same section, the highest variation ranges of major components prevailed at the time when the climatic change had the maximum effect. It is difficult to assess, therefore, if eustatic and climatic cycles or stronger current intensity would be the primary cause of the observed variations in lithologic cycles.

After 1 Ma, the enlarged land areas during lower sea-level stands may have resulted in more source terranes available for erosion. The Mesozoic and Cenozoic deposits of the emerged shelf may have resulted in a significant detrital input contaminating reworked micrite and clinoptilolite.

Before ~1 Ma, and particularly during the 1.5–1.8 Ma interval, significant occurrences of the ligneous phenols and, sometimes, of the cyannyl phenols, were observed. Such organic material likely originated from the grass savanna, indicating a maximum fragmentation of the forest block during this phase.

Despite the major 1.5- to 1-Ma hiatus, the recorded events of Hole 959C may be integrated into the postulated ocean-circulation history of the eastern Atlantic Ocean formulated by previous authors: 1.3 Ma would have been the time of the major deterioration of the climate, and ~0.9 Ma the intensification of the cold episode took place. It is proposed that major changes in deep-water circulation patterns had an influence on the time- and space-varying nature of the sediment equilibrium near the top of the margin crest of Hole 959C.

INTRODUCTION

Site 959 is located at 3°37.70′N and 2°44.10′W at a water depth of 2100 m on the landward edge of the Côte d'Ivoire-Ghana Marginal Ridge (Fig. 1). It offers the first opportunity of high-resolution analyses of the whole Quaternary of the Guinea Gulf (one of the empty areas of the Ocean Drilling Program [ODP] map). Previous paleoceanographic and paleoclimatic studies provided records that are more distant from the continent and, generally, deeper and farther north (ODP Leg 108 and numerous successive cruises of Lamont Doherty Geological Observatory, Woods Hole, and U.S. Naval Oceanographic Office vessels in the past four decades). In the Southern Hemisphere, the less-distant references for a whole Quaternary record are located near the Walvis Ridge (Deep Sea Drilling Project [DSDP] Legs 40 and 74–75). Ruddiman and Janecek (1989) argued that the more immediate control of the equatorial ocean is the subantarctic ocean, as suggested from late Pleistocene orbital variations (McIntyre et al., 1989). Subsequently, studies of cores from the equatorial Atlantic (and, if possible, from the Southern Hemisphere) are needed to check this probable connection.

Hole 959C was drilled on a small plateau that extends just north of the top of the Côte d'Ivoire-Ghana Marginal Ridge, on the southern shoulder of the Deep Ivorian Basin. Based on this special topographic location, one can expect that, in spite of a moderate distance

[1]Mascle, J., Lohmann, G.P., and Moullade, M. (Eds.), 1998. *Proc. ODP, Sci. Results*, 159: College Station, TX (Ocean Drilling Program).

[2]Laboratoire de sédimentologie et géochimie marines, URA CNRS 715, LEA Sciences de la mer, Université de Perpignan, Avenue de Villeneuve, 66860 Perpignan Cedex, France. giresse@univ-perp.fr

[3]Laboratoire de biologie végétale, Université de Perpignan, Avenue de Villeneuve, 66860 Perpignan Cedex, France.

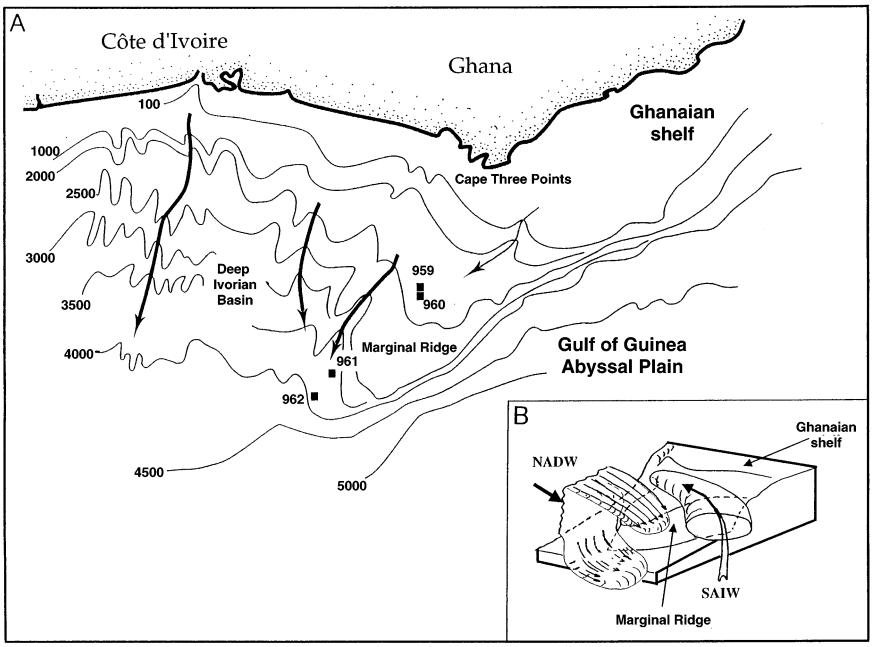

Figure 1. **A.** Locations of sites drilled during Leg 159 (contours in meters); arrows with thick lines indicate the major supply by gravitational processes, arrow with thin line marks the possible supply to Site 959. **B.** Scheme of interference circulation between North Atlantic Deep Water (NADW) and South Atlantic Intermediate Water (SAIW), according to Sarnthein et al. (1982).

from the shore (~120 km), only a minor part of the mass gravitational flow from the Ghanaian slope can reach Site 959, the major part of this flow being transported into the Deep Ivorian Basin. Consequently, the total thickness of Pleistocene sediment in Hole 959C does not exceed ~20 m (Shipboard Scientific Party, 1996). It suggests a Pleistocene Linear Sedimentation Rate (LSR) seven or eight times weaker than those recorded at the same water depth on the Gabonese Margin (Bonifay and Giresse, 1992) or three- to fourfold lower LSR than reported in the basin of the eastern equatorial Atlantic (deMenocal et al., 1993). It implies low LSR apparently similar to nearby Site 962 at 4737 m water depth, but exposed to gravity-induced supply.

The main focus of this study is the broad-scale evolution of paleoclimatic response at time scales longer than the primary orbital band (20–100 k.y). The paleogeographical potential of Hole 959C (Shipboard Scientific Party, 1996) stems from (1) its regular hemipelagic sedimentation without evidence for mass-gravitational flow, slumping, or other disturbance, (2) from its relative proximity to the shoreline, slightly uncommon in the ODP and DSDP records, (3) from its bathymetric largely above the depth-range trough in which Pleistocene dissolution has been important, and (4) from its location within a tropical area probably safe from major disturbance controlled by coastal upwelling as the high-productivity region of the Angola Basin (Van Bennekom and Berger, 1984) and eolian dust fluxes as over the northwest Africa margin (Sarnthein et al., 1982). However, modern but short seasonal upwelling along the Ivory Coast-Ghana margin is described (Voituriez and Herbland, 1982; Verstraete, 1992), and fluctuations may be expected during Quaternary, although with presumed lower amplitude than along the northwest and southwest African coast.

STRATIGRAPHY AND CHRONOLOGY

An initial biostratigraphic control was provided by shipboard analysis of calcareous nannoplankton, planktonic foraminifers, and silicoflagellates (Shipboard Scientific Party, 1996). This preliminary study approximated the Pliocene/Pleistocene boundary from 18.6 m below seafloor (mbsf) (Hole 959A) to 21.3 mbsf (Hole 959C). However, it seems that age assignments from each of the microfossils groups are too poorly correlated to provide precise estimations. Thus, in Hole 959A, this calcareous nannofossil boundary occurs near 18.6 mbsf, but the first occurrence of planktonic foraminifers that approximates the same boundary was found in Hole 959C as low as 24 mbsf using the CN12–CN13 subzones transition. However, potential ecological problems are envisaged to explain the lack of any indicator of subzone like CN13b (I.C. Shin, pers. comm., 1996).

Magnetostratigraphic ages (Shipboard Scientific Party, 1996) are consistently younger than the biostratigraphic ages. The offset between both sets of datum suggests inaccurate determination of magnetostratigraphic ages because of the low intensity of magnetization (Shipboard Scientific Party, 1996).

Thus, the stratigraphic control of Hole 959C was performed by means of oxygen and carbon isotope curves, which were established on tests of the epibenthic taxon *Cibicides wuellerstorfi* (G.P. Lohmann, pers. comm., 1996). Age fix points and corresponding depth levels used in this study are presented also in this volume (Wagner, Chap. 41, this volume). The data presented are from the uppermost three cores (21.3 mbsf). The combined isotopic data from the upper 12 m provide a record over the last 25 oxygen isotope stages. This curve indicates that mean sedimentation rates are very low and that two stratigraphic intervals are missing (Figs. 2, 3). Average mean LSR between 1 and 2 cm/k.y. are three to four times lower than those reported from deeper bottom depths or height times lower than those recorded at the same bottom depth on the Gabonese slope (Bonifay and Giresse, 1992). Two hiatuses were observed: a ~80 ka one ~1.5 mbsf and a major one (520 ka) around 11.9 mbsf. In each case, these hiatuses were preceded by a decreasing accumulation rate: respectively, 0.13 cm/k.y. at 1.5 mbsf and 0.61 cm/k.y. at 11.9 mbsf. The gap around 11.9 mbsf was previously suggested by correlation of magnetic susceptibility record (Shipboard Scientific Party, 1966).

METHODS

Samples about 10 mL in size were taken every 10 cm (2.5–5-cm intervals) throughout the upper 20 m of Hole 959C. They were taken at 0–2.5 and 5–7.5-cm intervals in some fluctuating carbonate-content curve sections of the upper Pleistocene. Samples were frozen on board and then freeze-dried in the shore-based laboratory. The organic and mineral carbon contents were obtained from dry weight sedi-

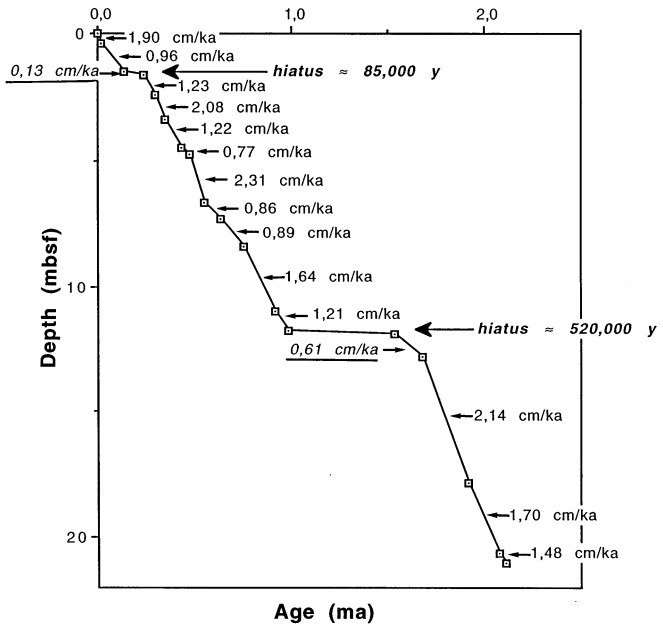

Figure 2. Mean sedimentation rate at Hole 959C based on oxygen isotope curve (Lohmann and Wagner, pers. comm., 1996).

ment by combustion in a Leco analyzer (after acidification of the sample with H_3PO_4 for total organic carbon). The $CaCO_3$ content of the total sediment was then calculated from the percentage of mineral carbon.

Sediment sample slices (4 cm long, 3 cm wide, and 0.5 cm thick) were taken on board and placed in small plastic boxes for microstructural analysis (laminae and scour contacts). In the laboratory, they were impregnated with resin to study microfacies in the thin section.

Bulk mineralogical data were obtained by systematic X-ray diffraction (XRD) measurement performed on untreated powder slides using a CGR θ60 with Co-anticathode. In this case, the results can be treated as a statistical approximation of the mineralogical composition.

These analyses focused mainly on the components of the sand and clay fraction and were performed on loose sediments after sieving with a 50-µm sieve. Sand component distribution was observed with the binocular microscope and, in some cases, with the scanning electron microscope (SEM). A part of this sand fraction was treated with 0.1.-N HCl to remove the carbonate and to calculate the insoluble sand fraction percentage, namely the percentage of green clay infilling in way of glauconitization. Further analyses were performed on green grains with an energy dispersive microprobe (TRACOR), coupled with the SEM and using XRD.

Grain-size characteristics of fine-grained samples (<50 µm) were obtained using a Sedigraph 5100. For each a 3-g bulk sample was prepared. The organic matter was removed using 30% diluted technical H_2O_2. After rinsing and drying, the sample was brought into suspension using 80 mL of demineralized water with 5 mL of a peptizing agent (1 g sodium hexametaphosphate in 1 L of water). Then the container was released to prevent settling of the sediment before being further analyzed.

The <2-µm particles were selected by sedimentation and then prepared in oriented aggregates. The XRD were made using (1) an untreated sample, (2) a glycolated sample, and (3) an occasional sample heated for 2 hr at 500°C. Semi-quantitative evaluation was based on the peak heights and areas (Chamley, 1980). In the near absence of chlorite, the heights of the 001 peak and of the 001 kaolinite (glycolated sample) were taken as a reference. Taking into account the poor and uneven crystallization of minerals, no corrections were applied. But, generally, this semi-quantitative estimation is diminished for the loose-crystallized minerals such as kaolinite.

Diffractograms of green grains were recorded using CoKα radiation as well. Several grains paramagnetically or hand picked were analyzed. The grains chosen for analysis were cleaned of the muddy matrix infilling fissures by ultrasonic bath and ground.

Elemental analyses of the organic matter was coupled with pyrolysis-gas chromatography-mass spectrometry (PY-GC-MS) and high performance liquid chromatography (HPLC) techniques, which, respectively, allow the identification of the major classes and individual compounds such as phenols. For the PY-GC-MS study, we used a CDS Pyroprobe 190 heated filament coupled directly to a HP 59995 gas chromatograph. Pyrolysis products were grouped into five main families: (1) aromatic hydrocarbons, (2) nitrogen-containing compounds, (3) sugars, (4) phenolic substances, and (5) amino sugars (acetamide). The HPLC method used an alkaline nitrobenzene oxidation technique to characterize the biological degradation products of lignins (Chen and Chang, 1989). The analysis of polysaccharides was realized according to the colorimetric method with anthrone.

LITHOLOGY AND MICROSEQUENCE VARIATIONS

The upper 20 m of Hole 959C comprises dark gray-green foraminifer ooze and nannofossil ooze with various admixtures of the two forming interbeds (Shipboard Scientific Party, 1996). Slightly lighter colors arise from increased foraminifer abundance. Two types of foraminifer concentrations were observed (Fig. 4):

1. Burrows 2–5 cm wide are scattered throughout, although these are rather concentrated below 13.8 mbsf. Some are filled with lighter colored, coarser ooze. This slight to moderate bioturbation produces gradational variation in color within the boundaries between the successive beds. Their occurrence may explain the apparently structureless deposit (e.g., 4–7 mbsf): the contacts have been smeared.
2. Layers (1 cm thick) have up to 60% foraminifers. They occur as 1-mm-thick parallel laminae or as individual laminae of various thicknesses and are scattered throughout most of the Pleistocene deposit. Only two scour contacts occur, at ~3.8 and 10.4 mbsf, with an increased concentration of foraminifers above them.

Various thin sections of indurated samples were made in the so-called bioturbated intervals. In various cases, these intervals display 1-mm to 1-cm laminae with increased concentration of foraminifers that produce too slight a color variation to be observed macroscopically. These thin layers of foraminifers present a porous structure with a sparse clay matrix mixed with micrites (probably inherited shelf sediment) and an increased amount of fragmented shells. In various intervals, their frequencies markedly increase to one per centimeter, indicating a slightly higher repetition than those observed at first sight. Based on a 1–2-cm/k.y. LSR for the upper 11.9 m of the hole, their dominant period has varied by as much as 1–2 k.y. This frequency is not consistent with a climatic forcing, but may be the result of contourite deposited during phases of pronounced bottom-current activity (Jacobi and Hayes, 1982). To the water depth of Hole 959C, interference circulations between southward-flowing North Atlantic Deep Water (NADW) and northward-flowing South Atlantic Intermediate Water (SAIW) or Antarctic Intermediate Water (AAIW) (Sarnthein et al., 1982) would be the more probable assumption (Fig. 1). The repetitive change in bottom-water intensity would be triggered by major pulses of Antarctic Bottom Water (AABW) or NADW as observed in Pleistocene cores of the southwestern Atlantic (Johnson, 1985). The two scoured (erosional) surfaces may result

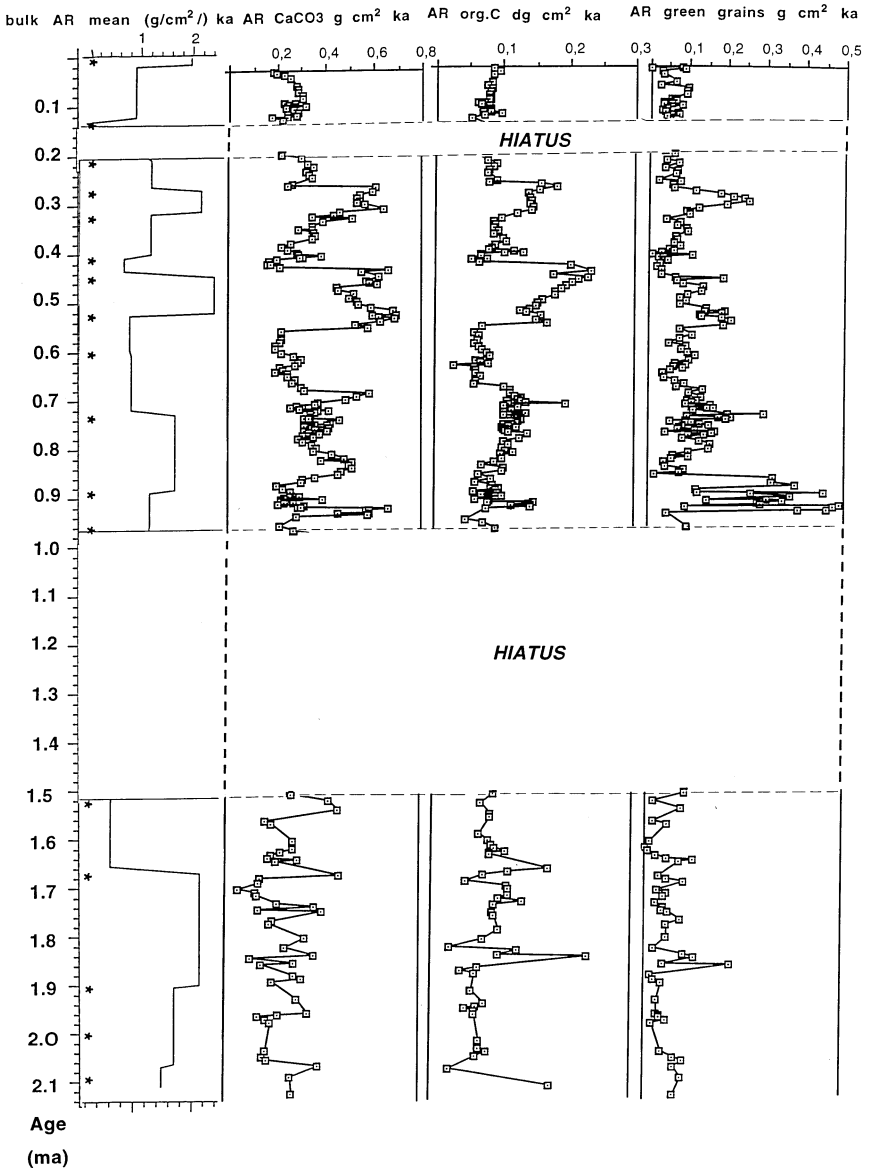

Figure 3. Mass accumulation rates of bulk sediment carbonate, organic carbon, and green grains for Hole 959C.

from the same paroxysmal depositional process, and the deeper one is observed just above the major hiatus of the stratigraphic column, namely at the end of an erosional discontinuity.

Many more glauconitic infillings of foraminifers were observed at ~11–12 mbsf, probably accounting at least in part for the interval's low accumulation rate (Giresse and Odin, 1973; Odin and Matter, 1981). One microsequence occurs over a 3–4-cm interval near 15 mbsf (Fig. 4C). The usual nannofossil ooze with foraminifers is succeeded uphole by a winnowing 1-cm-thick lag of foraminifers with some light green infillings. Above, another 1-cm layer was observed with several foraminifers filled with a darker green glauconitic matter. Other foraminifer shells were partly replaced by green material, and still others were partly coated by pyritic framboids as a result of late diagenetic overgrowths. Therefore, in this upper layer, a mechanical (winnowing) process of concentration of foraminifer shells was followed by a geochemical process of glauconitic neoformation. At Site 960 (2046 m water depth) on the top of the transform margin, the section is more condensed and eroded as a result of a focusing of the westward currents (Wagner, Chap. 41, this volume). But in the deeper Site 962 (4637 m water depth), sediment accumulation was also punctuated by numerous hiatuses, and the presence of several glauconitic hardgrounds suggests that the winnowing process of Hole 959C was probably enhanced.

It is therefore suggested that the persistently low sedimentation rate at Hole 959C was largely controlled by intensive winnowing and sediment redistribution caused by enforced bottom currents. This study also shows evidence to support the idea that downslope transport by gravity processes was absent during Pleistocene sedimentation.

GRADUAL TRENDS OF SEDIMENTATION OVER THE LAST 125 K.Y. (INTERGLACIAL-GLACIAL CHANGE)

In various previous studies (Berger and Winterer, 1976; Damuth, 1975; Hays et al., 1976; Morley, 1977; Morley and Hays, 1981), variations in biogenically produced $CaCO_3$ were used to reconstruct the oceanographic conditions in the South Atlantic (and in other oceans) in conjunction with oxygen isotope stratigraphic ^{14}C dates and foraminifer biostratigraphy. At 18 ka, the calcite-compensation depth in

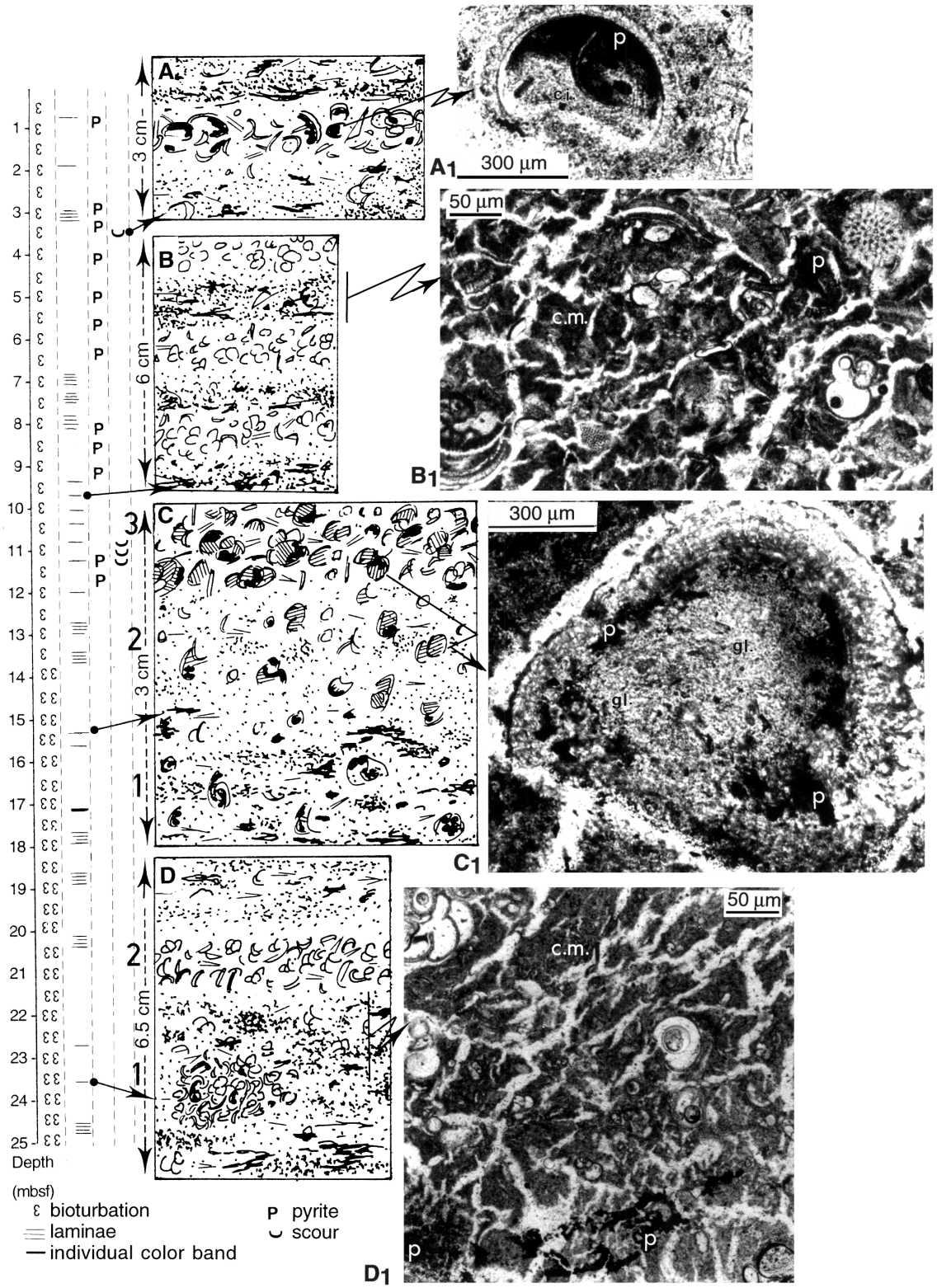

Figure 4. Selected microstructures and microfacies with regard to core-description forms (Shipboard Scientific Party, 1996). **A.** Scoured contact corresponds to an increased abundance of foraminifers (winnowing action); **A_1.** Loges are filled with light-gray clay (c.i.) and with pyrite (p), and f = foraminifer fragment. **B.** An observed single laminae corresponds in fact to three distinct and fine laminae with high content of foraminifers; **B_1.** Darker interbeds of organic clay matrix (c.m.) with pyrite-rich aggregate (p) and empty microtests and radiolarians (right corner) (the striped markings are related to induration artifacts). **C.** An upward microsequence with (1) a nannofossil ooze with foraminifers, (2) a foraminifer ooze with the beginning of test infillings, and (3) a glauconitic foraminifer ooze with glauconitic and pyritic infillings. **C_1.** Unfinished glauconitic infilling (gl.), then pyritic overgrowth (p) in the unoccupied void. **D.** A general overview of the sediment during a high sedimentation rate episode with test concentrations of (1) burrowing or (2) winnowing throughout. **D_1.** Microfacies present abundant pyritized vegetal debris (p) and a dark clay matrix (c.m.); microtests are generally empty.

the South Atlantic was approximately 400 m shallower than today between 0° and 42°S latitude, and during this last glacial maximum, the sea-surface temperatures in the eastern equatorial Atlantic were 3° to 5°C cooler than today (Morley and Hays, 1981).

Although the best time resolution was about 10 k.y., our carbonate record gives evidence of marine calcareous plankton responding to sea-surface temperature and consequent paleoproductivity. Because of the relatively constant bulk accumulation rate, dilution effects in the closed percentage system appear to be negligible. Both maximum (1.4 mbsf) and minimum (0.04 mbsf) concentrations indicate a continuous drift from the last interglacial (125 ka) toward lower percentages until the last glacial maximum (18 ka) (Fig. 5A). According to this trend, it is suggested that the upper part of the Holocene period would be partly missing.

The sand fraction (>50 µm) is almost completely composed of planktonic foraminifer tests. Its content (Fig. 5A) reaches values lower than 30% from 1.4 to 0.9 mbsf, then becomes lower than 15% in the upper part of the core section (except for one higher value at 0.14 mbsf). It is therefore suggested that carbonate accumulation was not exclusively controlled by the decrease in paleoproductivity, but was at least influenced by additional detrital inputs of very fine particles (<50 µm). Consequently, the sandy fraction curve would be a better tool of reconstruction in paleoproductivity here. At the first part of Stage 3, green grains demonstrate various content peaks, and Stage 5 is marked by a percentage depression. Contents of organic carbon are roughly opposite to that of $CaCO_3$ and sandy fraction curves. The percentages increase slowly upward from 0.9% to 1.1% to more than 1.3%. The exact cause of these fluctuations has not yet been completely resolved; as many as two factors control the total organic carbon at this period: (1) terrigenous organic carbon supply, and (2) marine productivity of planktonic organisms. Various studies of eastern equatorial Atlantic sediments (Sarnthein et al., 1981; Jansen et al., 1984; Pokras and Molfino, 1986; Jansen and Van der Gaast, 1988; Stabell, 1989; Tiedemann et al., 1989; Bonifay and Giresse, 1992) showed the onset of enhanced trade winds via an onset of coastal upwelling activities during the glaciation period. Low sea level largely occurred during the last glaciation with prominent minima between 12 and 24 ka and between 61 and 74 ka (Damuth, 1975). The diffractometric ratio of quartz to kaolinite was measured for each bulk sample and plotted against depth; the values are slightly uneven, but the highest are observed in the interglacial episode of Stage 5. The gibbsite, inherited mineral from the ferrallitic soils developed under the intertropical climate, also reaches higher amounts during Stage 5.

In response to the sea-level minima, erosion of Mesozoic–Cenozoic deposits of the shelf was enhanced and thus erosion of Precambrian outcroppings on the present shore was faster during sea-level maxima. The clinoptilolite, a diagenetic zeolite, is common in various Tertiary sediments of the area (Robert, 1982; Stein and Faugères, 1989; Shipboard Scientific Party, 1996), its presence in small amounts in certain deposits (0.24–0.54 mbsf) of the sea level minima fits into this general scheme. Green grains of the glauconitic facies, here test infillings, appear to form during a synsedimentary period of slackening in the accumulation rate (Odin and Fullagar, 1988). Its percentage curve is slightly uneven, but the percentage depression apparently correlates with isotopic Stage 2.

Geochemical analysis of phenol compounds and particularly lignin oxidation products adds complementary information to the organic fluxes (Fig. 5B). The phenol contents greatly decrease upcore, roughly parallel to a decrease in hydroxybenzyls. On the other hand, the syringyl-vanillyl ratio (S/V) tends to increase upward because the syringyl phenols are more fragile than the vanillyls (Hedges and Mann, 1979). In this general trend, the climatic optimum (Stage 5) is

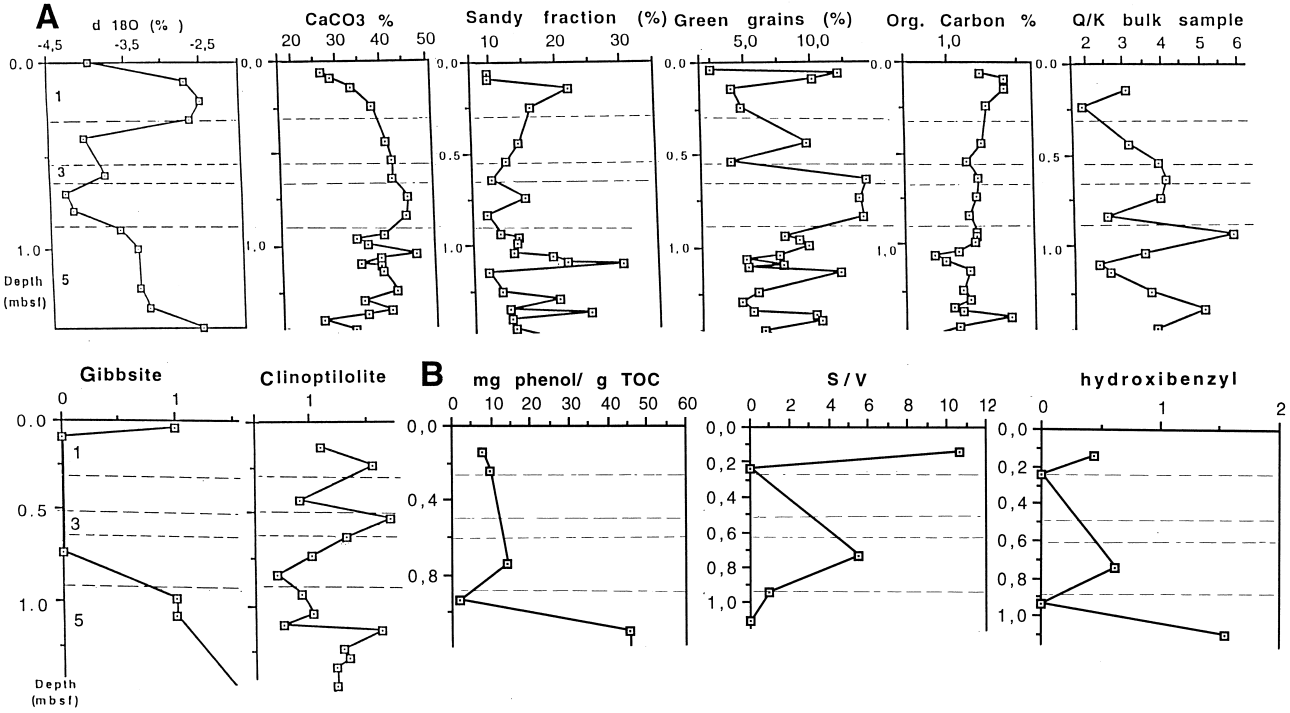

Figure 5. (A) Sedimentary and (B) geochemical evidence of climatic change at Site 959 for the last glacio-eustatic cycle. **A.** Oxygen isotope curve, contents of $CaCO_3$, sandy fraction, green grains (in percentage of the sandy fraction), organic carbon (in percent of the bulk-sediment sample), and quartz:kaolinite ratio; the clinoptilolite and gibbsite data are expressed as an XRD intensity ratio of clinoptilolite/4.26 Å quartz and gibbsite/4.26 Å quartz. **B.** Selected compound abundances of organic matter: phenol (in mg/g dry sediment), S/V (syringyl vs. vanillyl), and hydroxybenzyls (in percent of the phenols).

reflected essentially by cellulosic compounds derived from leafy matter, whereas the climatic deterioration is indicated by the accumulation of more degraded and more steady material (ligneous-type).

This attempt to determine a lithostratigraphic cycle fits into the general scheme of the last glacio-eustatic cycle (without a part of the Holocene record) where climatic and eustatic parameters showed major variations. However, some variations do not appear to be directly related to these glacial/interglacial cycles because of limitations by the time resolution is obtainable from low sedimentation rate and because of the presumed winnowing interference. Within a broader scale of observation (10^6 yr), the older fluctuations would not be explained so schematically with regard to the reconstruction of the paleoceanographic history.

LONG-TERM TRENDS

Carbonate and Coarse-Fraction Analysis

The sand fraction is almost exclusively composed of whole or broken foraminifer tests (mostly pelagic) without any quartz grain. However, we observe that the sand fraction and $CaCO_3$ records (Fig. 6) are sometimes significantly different and that the positive relation is poor (R2 = 0.23). This relation is dependent on development and concentration of green clay and silt-sized quartz infillings of microtests. Another cause of nonparallelism of the two curves is attributed to the presence of nearly half of the carbonates in the fine fraction (<50 µm). These fine carbonates are mostly composed of microfragments of planktonic foraminifers in the 25–50-µm fraction and also of micrites invisible using SEM and only detected using microprobe. These micrites are closely associated with the clayey matrix.

The Pleistocene carbonate curve can be divided into two parts:

1. The upper 11.9 mbsf correspond approximately to the last 0.99 m.y. (based on oxygen isotope curve). Relatively high carbonate contents (35%–40%) characterize this upper part. At first sight, the wider fluctuations (with a deviation near 20%–25%) appear to correspond to the timing of glacial/interglacial climatic cycles (Fig. 6). However, several glacial stages (22–24, 16, 12, 10, 8, and 4) show high carbonate and sand contents. Such records are not consistent with either those from pelagic sections of the equatorial Atlantic (Damuth, 1975; Jansen et al., 1984; Verardo and McIntyre, 1994), or with the values of the last interglacial-glacial change of Hole 959C. Bulk calcium carbonate mass accumulation rates closely follow bulk mass accumulation (Fig. 3) and do not appear to be directly related to paleoproductivity.

2. Below 11.9 mbsf, the carbonate content generally ranges between 10% and 30%, but always with large variations (deviation near 20%). Elevated contents of carbonate suggest a closer connection to the interglacial period than in the upper section; sand and carbonate values allowed positive correlation (Fig. 6). Paleoproductivity-driven formation of carbonate and sand cycles was likely forced by orbital cycles, although the oscillation of the curves is not strictly connected to glacial/interglacial cycles. Variations in mass accumulation rates reveal changes in much longer time scales than the carbonate and sand cycles (Fig. 3).

The carbonate-content curve of the fine fraction roughly parallels the two sections of the carbonate-content curve. Both emphasize the 11.9-mbsf boundary (core break 2/.3; Fig. 6). The two variables present a slightly good coefficient correlation ($R_2 = 0.67$). A detailed observation of timing fluctuations of the two curves provides evidence for a frequent parallelism below 11.9 mbsf indicated by a fine fraction very nearly without carbonate. Above, this parallelism is partially altered; this change is mainly connected with the increased

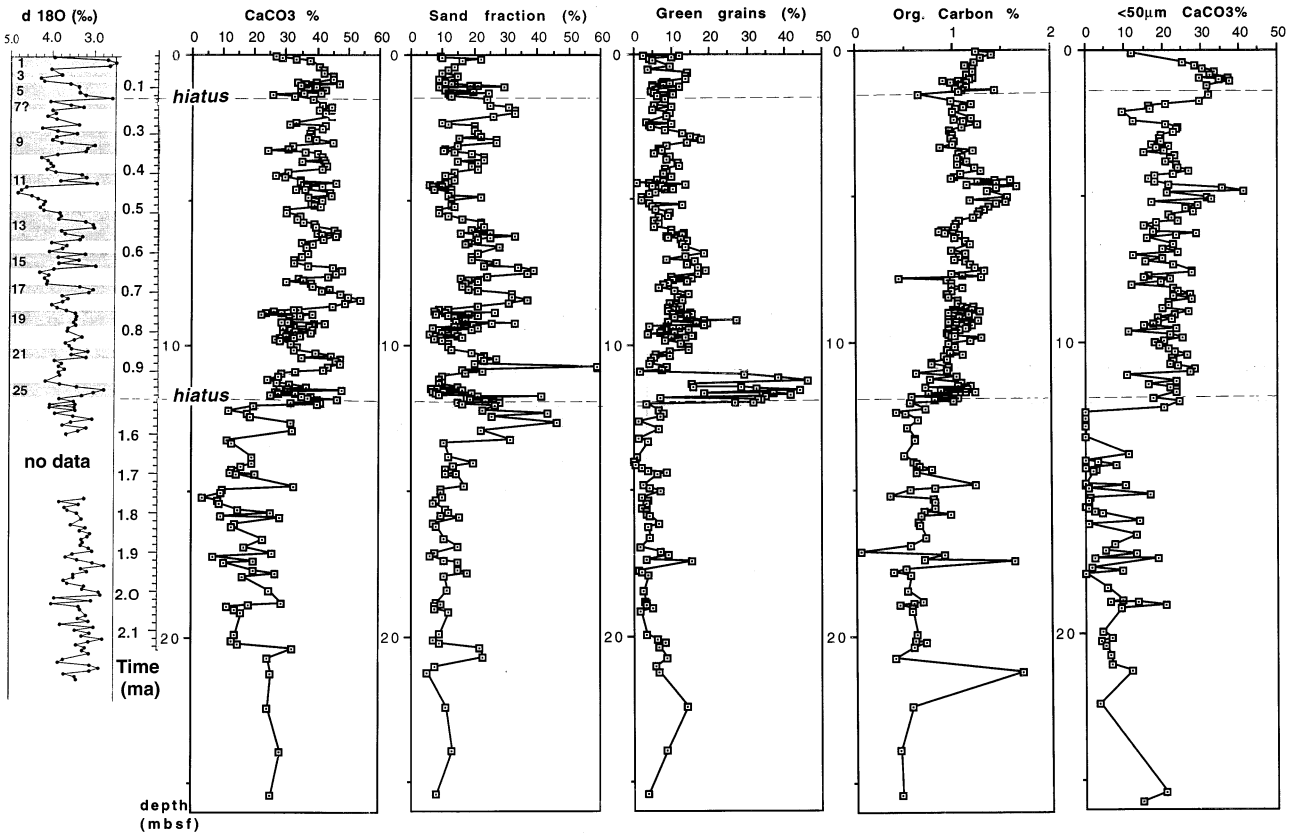

Figure 6. Downhole profiles for Hole 959C of the main lithologic compounds (in percent dry sediment).

fragmentation of planktonic foraminifers above 11.9 mbsf. The reason for this increase can be twofold: (1) the enhanced bottom water currents after 1 Ma would be consistent with the fragmentation increase, and (2) larger climatic fluctuations during the Brunhes Chron were inferred from combined effects of 10- and 40-k.y. periods.

The consequent wider eustatic fluctuations emphasized erosional processes of the Cenozoic calcareous deposits of the mid-shelf (Blarez, 1986) during low sea-level stands. In addition to the bioclastic accumulation, very fine micrites reworked from the outer shelf appear to account for the anomalous relationships observed in the upper 11.9 mbsf. The two effects might be superimposed. However, within this broad-scale study, we have no evidence for a correlation between interglacial period and a better preservation of the microtests.

Clay Minerals and Other Mineralogical Indicators

Detailed XRD analyses suggest that during the last ~2.4 m.y., a relatively constant background of clay mineral deposition has existed (Fig. 7) on which eustatic oscillations in accessory minerals are superimposed. The major mineral components found in the clay-size fraction (without weight correction) are quartz, calcite, and the clay minerals kaolinite (45%–50%), montmorillonite (35%–40%), and illite (10%–15%). Occurring in minor quantities are gibbsite, clinoptilolite, pyrite, and feldspar. The relative abundance of the clay minerals is in good agreement with various previous works (Biscaye, 1965; Griffin et al., 1968; Bowles, 1975). Cold and warm periods were analyzed; no significant changes in the relative abundance of the clay minerals were found, suggesting that the climatic changes of the Pleistocene had little effect on the production and deposition of clay minerals in this margin. At most, we note a slight increase of montmorillonite during the early Pleistocene time and maybe during the 0.5–2.5-mbsf interval. The outstanding exception is the illite percentage curve: the small changes in content of this mineral are particularly interesting, considering the other changes found in this Hole. The illite content (Fig. 8) has slightly increased above 11.9 mbsf with the higher amplitude of fluctuations. This change may result from increased reworking of Mesozoic–Cenozoic deposits during low sea stands rather than a significant climatic forcing. Illite is a slightly abundant clayey mineral in West African Mesozoic and Cenozoic deposits (Robert, 1982). For the most part, the highest content of illite parallels the glacial stages (4, 6, 12, 16, 20, and 22), but some of them correspond to interglacial stages (13, 21, and 25)

One of the preliminary working hypotheses was a possible quartz supply from the Sahara desert or from the northern Chad area by the northeast Trade Winds to this southern boundary. Bowles (1975) in the eastern equatorial North Atlantic (4°–9°N) compared quartz/illite variations of the bulk sample with paleotemperature variations and suggested that major inputs of quartz correlate with cold periods. Our purpose was to apply the same method in our more intertropical environment. Because the 5.0 Å illite peaks were often of weak intensity, the peak heights of 7.15 Å kaolinite and of 3.34 Å quartz were used to estimate the quartz content variability. These ratios have relative, but not absolute, significance, and the hypothesis that they reflect changes in the abundance of quartz rests on the general assumption that the kaolinite abundance has not widely changed within the clay mineral set. The quartz/kaolinite ratios show large fluctuations (1–6), but there is not a clear relationship with time (Fig. 8). The higher values are noted after 1 Ma, but in fact, it is mainly the maxima values that are higher. A perfect peak-to-peak correlation with the cold isotopic stages is not observed. Some peaks appear broader or weaker than their counterparts; however, in most of the cases up to 11.9 mbsf, the quartz/kaolinite peaks correspond to glacial stages (4, upper part of 8, 16, 18, and 20; exceptions are 11, 17, and 25).

Clinoptilolite was detected by XRD in both of the grain-size fractions <2 µm and 2–50 µm. Also, small amounts of this mineral were detected in nearly all bulk samples of the Pleistocene. However, the

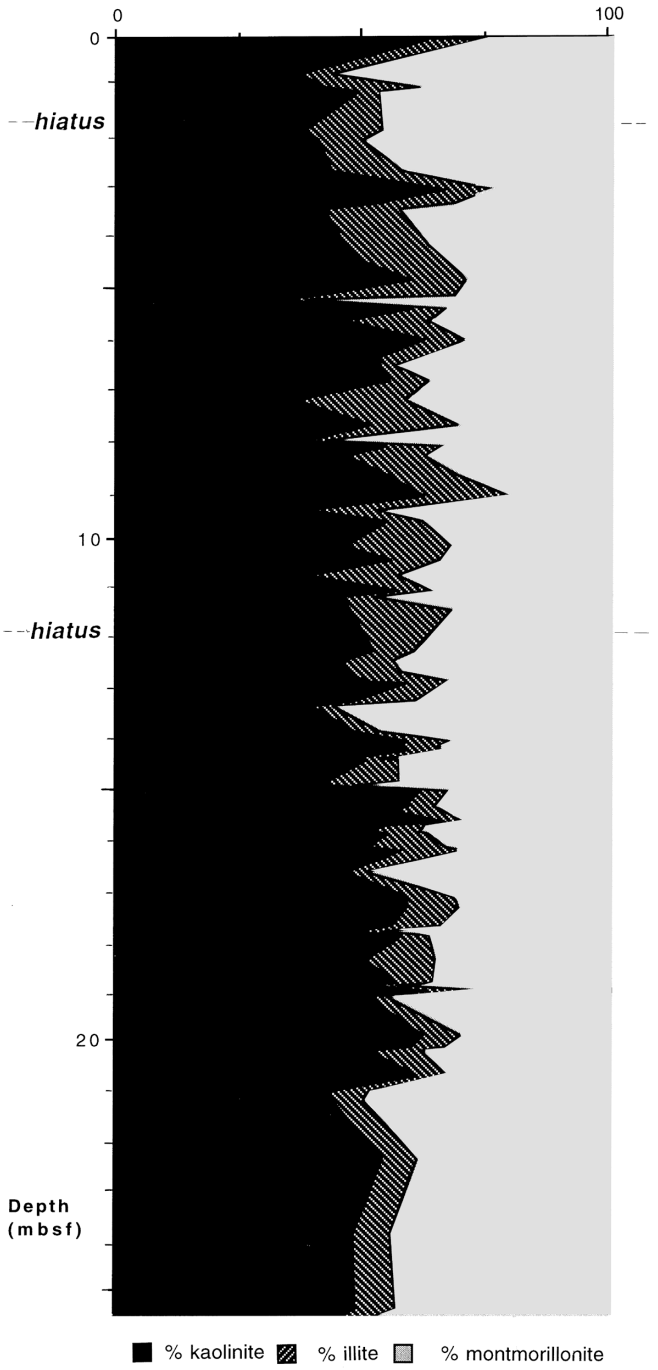

Figure 7. Vertical distribution of major clay minerals in uppermost 25 m of Hole 959C; mixed-layered clay (mostly montmorillonite illite) is included in the montmorillonite content.

best definition of the clinoptilolite (9.05–8.97 Å and 7.93–7.89 Å) was observed in the <2-µm fraction where the peaks frequently were associated with cold isotopic stages (3, 8, lower part of 10, upper part of 15, and lower parts of 16, 18, 20, and 26) and low sea-level phases with Cenozoic deposits reworking from the emerged shelf (see above). Amounts of this mineral inversely paralleled the kaolinite mostly after 1 Ma (Fig. 7). This suggests alternation of humid, high sea-level with low sea-level phases. Also, $CaCO_3$ contents of the <50-µm fraction were correlated with several cold isotopic stages (4,

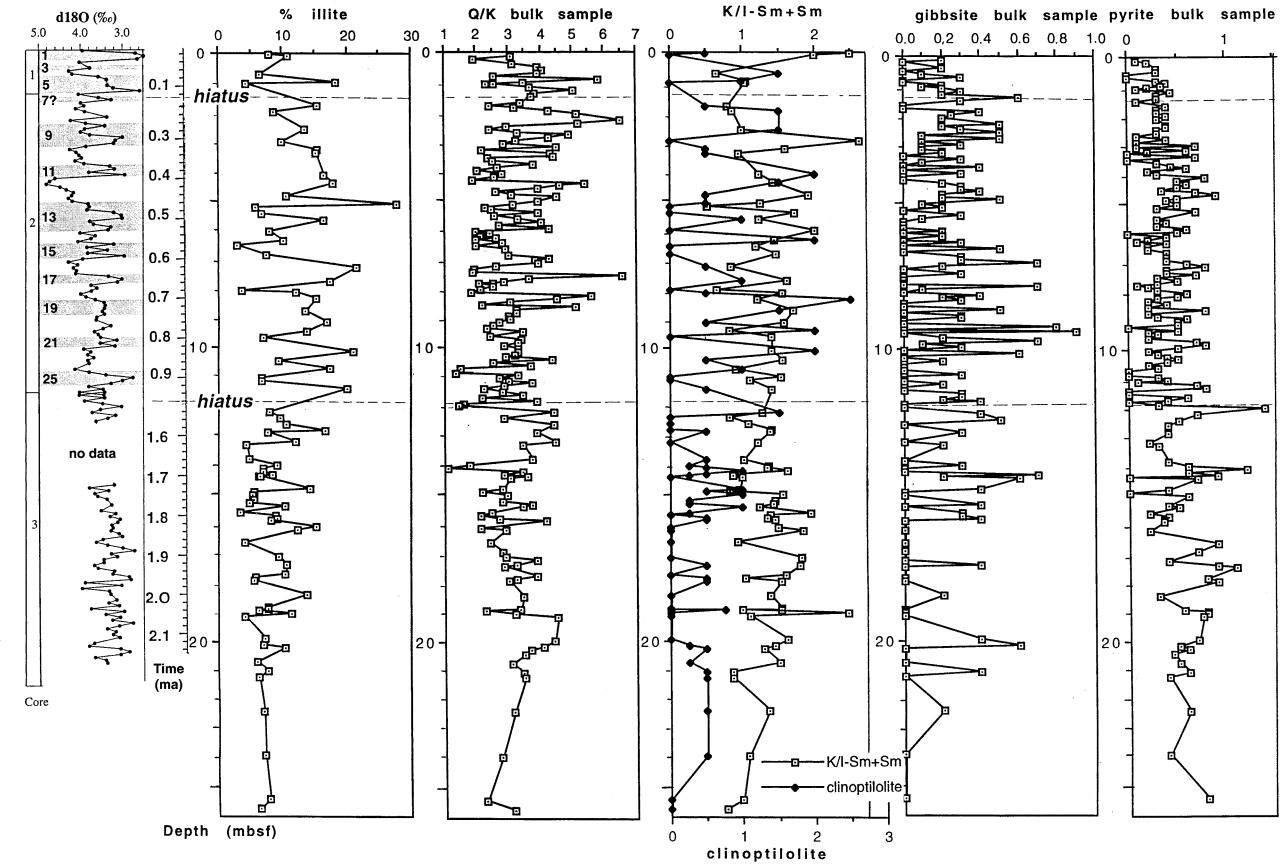

Figure 8. Clay minerals and accessory minerals for Hole 959C. Illite contents and K/I–Sm + Sm were performed on clay-sediment fraction; relative X-ray diffraction intensities of quartz (3.34 Å), gibbsite (4.82 Å), and pyrite (2.71 Å) were performed on bulk-sediment fraction.

8, 10, 14, top of 16, and 22) and considered as micrites reworking from the shelf. In this way, the increase of eustatic oscillation after 1 Ma and, consequently, of the erosion of the shelf, may be reflected by the uneven upward increase of clinoptilolite and micrite.

Very small amounts of gibbsite were recorded in the clayey fraction and in the bulk samples of nearly all the 20–25 m studied without any significant correlation. However, this mineral shows an irregular increase in the uppermost Pleistocene where the climatic oscillations are presumed higher: cyclic increases appear related to wet interglacial periods (Stages 5, 9, 11, 15, 17, 20/21 boundary, and 27). Pyrite was commonly observed as individual framboids or as late overgrowths on the glauconitic infillings. Its content presents a relationship apparently opposed to that of the glauconitization process. Based on XRD results from bulk samples (Fig. 8), the temporal distribution of pyrite suggests that in the lowermost Pleistocene, slightly higher concentrations are related to better burying and preserving conditions.

Green Grain Fraction

The green clay material was only rare in the form of free or full grains. The green pigments usually fill the chambers of the globigerine or buline or other pelagic foraminifers. Some grains correspond to the internal molds of the radiole of holothurids. Ellipsoidal fecal pellets only are rare. This material is devoid of any littoral evidence and cannot be interpreted as perigenic, transported from the top to the bottom of the slope. After decarbonatization, the sand fraction is mostly composed of the green infillings with small proportions of pyrite. When it was weighed and related to the bulk sand fraction, it became evident that green grains' abundance does not appear constant with time (Fig. 6), suggesting low content (<10%) below 12 mbsf and higher contents above this depth. Particularly, the 11–12-mbsf sand fraction presents the highest concentrations (20%–45%). Above 11 mbsf, green grain contents are commonly higher than 10%. As the sand fraction is mostly composed of carbonate microtests, it was previously suggested that the presence of green material must be related to this sand fraction, but it was observed that this relationship is not confirmed. In contrast to this assumption, green grains are sometimes more abundant in levels with low sand contents (e.g., 11 and 11.5 mbsf). The mass accumulation rate of green grains apparently show a poorer relationship with the bulk mass accumulation than the carbonate curve (Fig. 3). This distinct difference possibly suggests that green grain crystallization was not a synsedimentary process, but implied diagenetic cationic exchanges with overlying fluids. The green grain record shows repetitive maxima that are poorly related to glacial/interglacial isotopic Stages 3–4, 9, 14, 16, 19, and, especially, 24–25. Consequently, it is suggested that the 11–12-mbsf accumulation period corresponds to the slowing down of the erosional process after a long period of maximum bottom-water activity.

Generally, the lower contents of green grains correspond to white to pale green infillings that contain a small potassium content (1.41%–3.87% K_2O), an irregular content of iron (29.7%–42.7% Fe_2O_3), and a slightly high alumina content (7.22%–8.92% Al_2O_3) (Fig. 9). In contrast, higher potassium and, roughly, iron contents are related to pale green to green infillings, which are sometimes more or less split by fissures and cracks: respectively 4.6%–6.8% K_2O,

45.6%–52.7% Fe_2O_3, and 3.4%–5.2% Al_2O_3 for alumina. In the same levels, green to dark-green grains with deep cracks are widespread and sometimes abundant, especially in the 11–12 mbsf interval, the contents obtained were as follows: 7.14%–8.79% K_2O, 44.7%–55.04% Fe_2O_3 and 2.51%–3.26% Al_2O_3. The sediments richest in green pigments are usually very poor in pyrite, and the poorest present various pyritic molds and even in the early Pleistocene abundant pyrite framboids.

It is worth noting that whichever the apparent step of evolution, the grains give an XRD pattern (Fig. 10) with a restricted number of diffractions: 001, 020 (particularly developed), 112, and 003. This is characteristic of a disorder in the crystallographic structure. Accurate identification of this clay is a current analytical problem as separation and concentration of green grains require much more sample material than is available. The frequent heterogeneity of the associated phases (neoformed smectites and inherited products) and their poor crystallinity constitute difficulties to follow the precise definition of the evolution. However, we can recognize white or pale green grains with kaolinite associated with smectite and the darker green grains where all analyses show the absence of kaolinite and the increasing amount of smectites (forming cabbage-like structures) and interlayered structures. In any case, 10 Å phases were observed.

Such green grain concentrations (10%–40% of the sand fraction, 0.5%–15% of the bulk sediment) are unusual deeper than 2000 m water depth. In this case, weakness of detrital input and, especially, winnowing, produced accumulation rates that prevent a too rapid burial. Grains seem exposed at the sediment/water interface for periods sufficient to allow glauconitization. However, at these water depths, a latitudinal effect is also possible; a general relationship between continental iron influx to the slope and Pleistocene tropical climate can be proposed, particularly during the last 0.9 k.y.

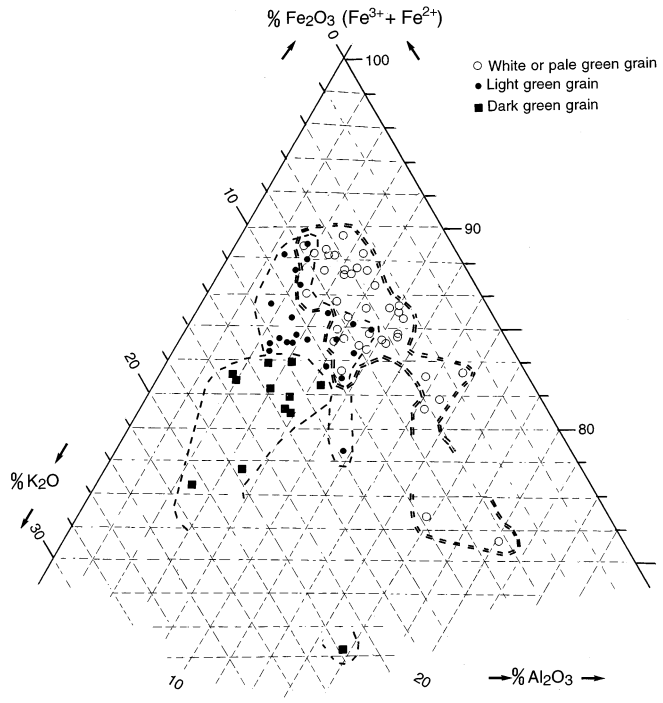

Figure 9. K_2O-Al_2O_3-Fe_2O_3 plot of microprobe analyses of various green grains where all iron is calculated as Fe^{3+}. The K_2O-Al_2O_3 coordinates present a sequence as a function of glauconitization intensity. The Fe_2O_3 values are irregularly scattered throughout the field.

Textural Characteristics of the Fine-Grained Fraction (<50 µm)

As the sand fraction is composed exclusively of foraminifer tests and their infillings, the analyses were performed on loose sediment after wet sieving with a 50-µm sieve. Consequently, these analyses focused mainly on the siliciclastic components related to hydrodynamic processes, but included both biogenic (broken tests) and clastic (micrites) 0%–40% $CaCO_3$ and, eventually, opal components. The analyses took into account the mode, the content of clay fraction (<2 µm), and the shape of cumulative frequency curves. Grain-size distributions of the sedimentary column exhibit globally a rather fine-grained assemblage. Typical modal or median values in the range of silt characteristic of basal deposits (40–20 µm; Faugères et al., 1989; Kounkou and Barusseau, 1988) of a turbiditic layer are wholly absent.

However, the grain-size assemblage is not devoid of any hydrodynamic signal. The distributions display a variation between log-normal curves (sigmoidal shape) corresponding to sediments submitted to a certain extent to sorting processes, and hyperbolic curves (Rivière, 1977) corresponding to sediments settled in a very quiet environment. Between these two limits (1 and 5; Fig. 11), other arbitrary types were distinguished in order to take into account the occurrence of different reported cases: (1) lower sorting of a sigmoidal distribution (4; Fig. 10) and (2) "logarithmic" distribution with low (3) or high (2) clay content (Fig. 11). Five grades of dynamic intensity were described; the lower the value, the more reduced the hydrodynamic activity and the more prominent the settling processes by decantation. This gradation emphasizes a vertical succession (Fig. 12) in which we may recognize the following:

1. From 25 to 19 mbsf, conditions correspond to uniform and active sedimentation, except for some increases in bottom dynamic processes at ~20–21 mbsf. The high modal values (10–15 µm) at ~21–24 mbsf are evidence of the settling deposition of very fine silts.
2. From 19 to 15 mbsf, an increase in bottom dynamic intensity is indicated; this coarser material is characterized by a mode ranging from 10 to 15 µm. This interval is mostly included within the high accumulation rate period of 1.9–1.67 Ma (Fig. 3) and seems to be deposited under bottom-current control.
3. From 15 to 11 mbsf, sediment is generally more finely grained, with an increase of the clay fraction. Quiet water conditions seemed to prevail during this interval, characterized by a slowing-down of the accumulation rate and by the deposits of abundant ligneous phenols and higher amounts of cynnamyl (see below). Just after a short episode of stronger bottom circulation (13–12 mbsf), the lowest decrease of accumulation rate (0.61 cm/k.y.) is suspected to be related to the paroxysm of winnowing activity. Therefore, these reworkings are a probable cause for the concentration and glauconitization processes of the clayey infillings.
4. Above 11 mbsf, the sedimentation is marked by maximum amplitudes of climatic and sea-level variations. Against a generally moderate accumulation rate, one can observe a relative turbulence decrease from 11 to 3 mbsf, then a higher current activity again during the last climatic cycles (above 3 mbsf). This last interval coincides both to the drastic slowing down of the linear sedimentation rate (0.13 cm/k.y.) and then to the second hiatus (≈85 ka) of the stratigraphic column. Maximum grades of dynamic intensities are not very closely related to the isotopic stages, but seem to be frequently correlated with glacial periods (Stage 2, transition 6–5, and Stages 8, 12, 16, 22, and 26). It is therefore suggested that the sand size of deposits was not mainly controlled by changes in continental input during the wet and humid period, but, at least, was largely influ-

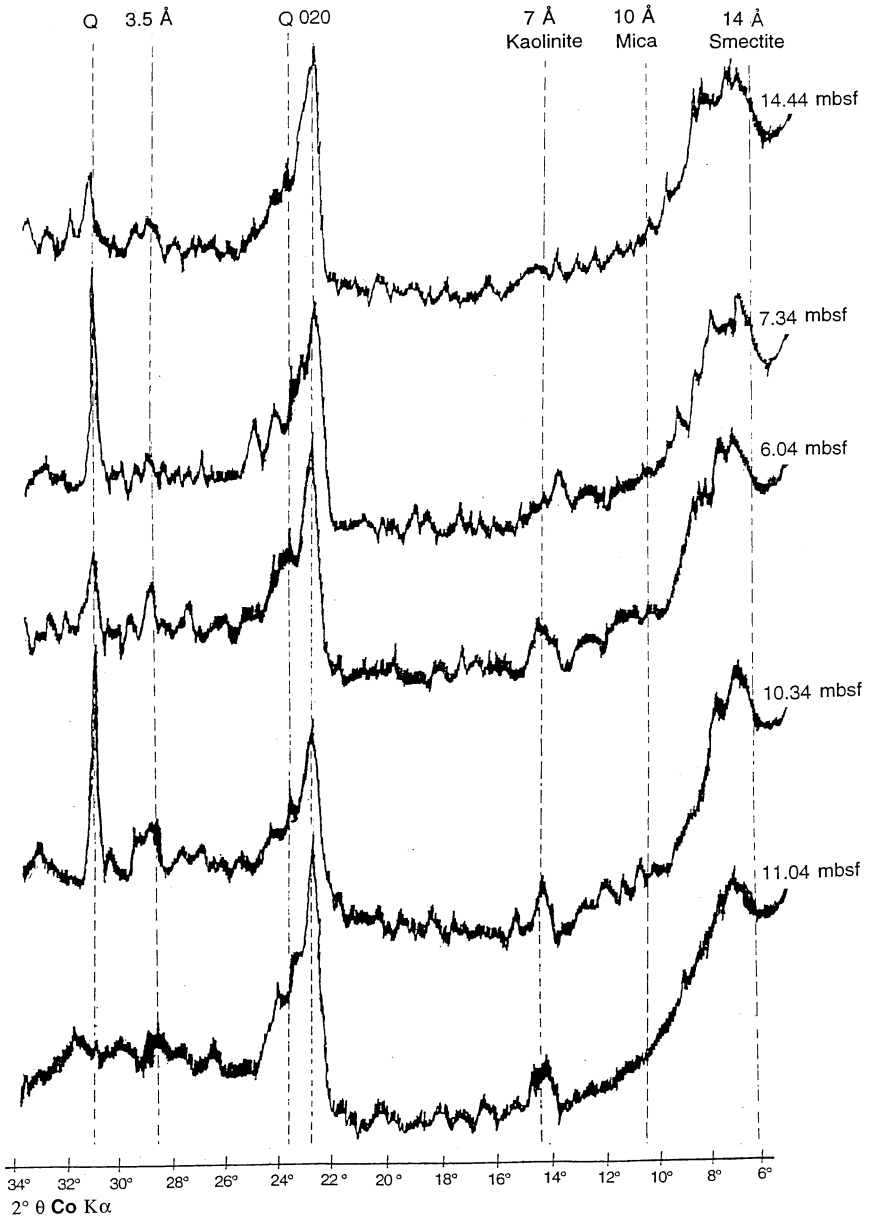

Figure 10. X-ray diffractograms of unoriented green grains. Examples were selected to show the decrease of inherited kaolinite vs. the increase of neoformed smectite and associated mixed-layered clays.

enced by bottom-current activities. Such an activity would be rather enhanced during glacials and closely associated with major pulses of deep waters.

Organic Matter and Biomarkers

The long-term trend of organic carbon content shows a general downhole decrease during the Pleistocene from 1.6%–0.8% to 1%–0.6% (Fig. 6). It is usually suggested that such a decrease has been primarily controlled by a diagenetic degradation linked to the burial depth. However, a slight yet identifiable boundary is observed around 11.9 mbsf (core break 2/3), corresponding to the higher/lower carbonate boundary: organic carbon mean values decrease from about 0.9%–1.5% to 0.4%–0.7% above and the entire curve is marked by fluctuations. As it was observed for the last glacio-eustatic cycle, the high-amplitude variations of organic carbon do not necessarily coincide with those of the carbonate fraction. Whereas the relation between these two parameters is slightly poor (R2 = 0.28; n = 231), mean accumulation rates for organic carbon closely follow the bulk accumulation rate records. However, on the one hand, variations in organic carbon contents do not appear to be directly related to glacial/interglacial cycles. On the other hand, in sections younger than Stage 5 and older than 0.9 Ma, elevated levels suggest a connection to a glacial period. As quantitative estimates of marine organic matter range from 15% to 60% (Wagner, Chap. 41, this volume) and as significant contributions of fluvial material to Site 959 are improbable, an elevated content of organic carbon during glacials can only be associated with wind-induced coastal upwelling off the Ivory Coast-Ghana (Verstraete, 1992). In the younger section (0.9–0.1 Ma), cyclic variation in organic carbon content is not obvious; only in some cases is there a relationship between high organic carbon content and interglacials (Stages 11, 15, and 25), but several climatic optima are not documented. This would imply frequent interference between accumulation and intensive sediment sorting and redistribution.

Progress in analytical methods has allowed the study of the origin of organic compounds globally photosynthetical products present in an ecosystem (Scribe and Bourdier, 1995). Marine ecosystems collect allochthonous organic matter from erosion or leaching of soils

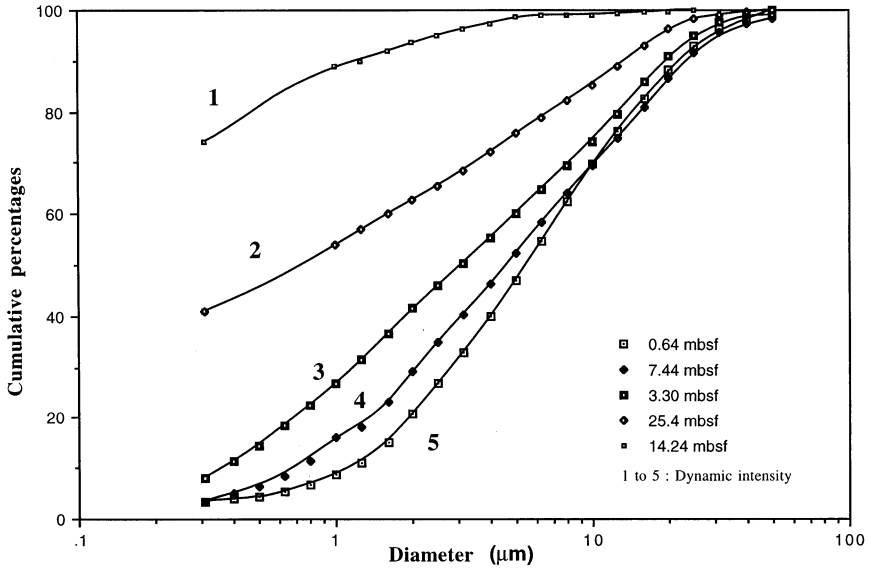

Figure 11. Typical grain-size assemblages (cumulative curves) showing the gradation between sorted (5) and unsorted (1) distributions. Three intermediate arbitrary cases were recorded along the section (2, 3, and 4).

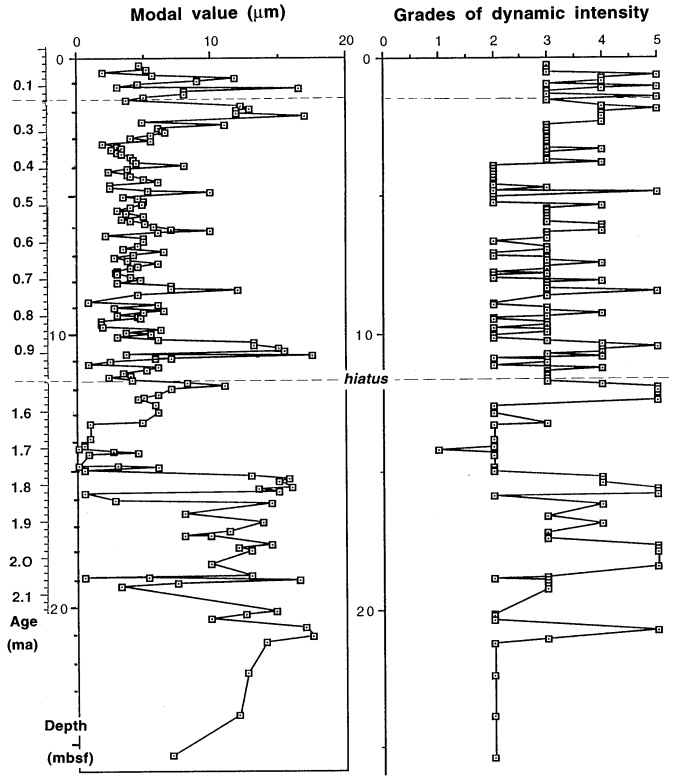

Figure 12. Grain-size mode and grades of "dynamic intensity" vs. depth.

admixed with autochthonous compounds produced by organisms living in the milieu.

Analytical methods are of two types: global or separative. We chose, for the first method, the colorimetry of polysaccharides and global analysis of sediment by Pyrolysis-Gas-liquid Chromatography coupled with Mass Spectrometry (PY-GC-MS), and for the second method, the analysis of lignin-derived phenolic compounds by high performance liquid chromatography (HPLC).

Polysaccharides

Moreover, the analysis of polysaccharides by a colorimetric method (Gallali, 1972) allows some information about the biodegradable material included in the deposits to be compared to resistant compounds such as phenols.

The distribution of polysaccharides (%C Poly/C_{org}) shows a general trend marked by a downhole decrease, certainly consecutive to diagenetic effects (Fig. 13). The concentrations decrease rapidly in the first meter. The values are then similar up to 7.8 mbsf. They increase from 8.4 to 17.4 mbsf, with the highest concentrations at 13.2 and 17.4 mbsf, which correspond closely to the major influxes of phenolic compounds (see below). Downward, the contents greatly decrease from 18.9 mbsf to the bottom (diagenetic effect).

Phenolic Compounds

Very few methods allow a precise determination of the origin of the organic matter, (i.e., whether it is autochthonous or allochthonous) because all of the organic characteristics depend at the same time on the origin and on the degradation intensity. In order to determine the relative importance of autochthonous and allochthonous organic matter, lignins can be used as biomarkers of the allochthonous organic fraction because they are secondary products produced exclusively by higher plants (Creighton et al., 1944; Towers and Gibbs, 1953; Freudenberg and Neish, 1968; Sarkanen and Hergert, 1971; Harborne, 1964, 1980) and are not significant components of lower plants (Farmer and Morrison, 1964; Siegel, 1969; Lewis and Yamamoto, 1990). Moreover, lignin analysis shows a phenolic monomer composition characteristic of the main taxonomic groups (Pearl, 1942; Creighton and Hibbert, 1944).

The method of lignin analysis adopted here is the cupric oxide alkaline oxidation of air-dried sediments. Separation and determination of phenolic monomeric units are achieved by HPLC (Hartley and Buchan, 1979; Serve et al., 1983; Serve and Piovetti, 1984). In the bulk of the 28 compounds measured, 11 represent (after Hedges and Ertel [1982]) the monomeric constituents derived from lignin by copper oxide oxidation. Three series can be cited: 4-Hydroxybenzyl (H), 3-Methoxy-4-Hydroxybenzyl (Guaïacyl or Vanillyl [V]), and 3.5-Methoxy-4-Hydroxybenzyl (Syringyl [S]). Each of these series presents an alkyl side chain with 1, 2, or 3 carbons. The compounds in C_6-C_1 can present the acid or aldehyde function, those in C_6-C_2 are ketons, and those in C_6-C_3 are acids. The last ones with a phenylpro-

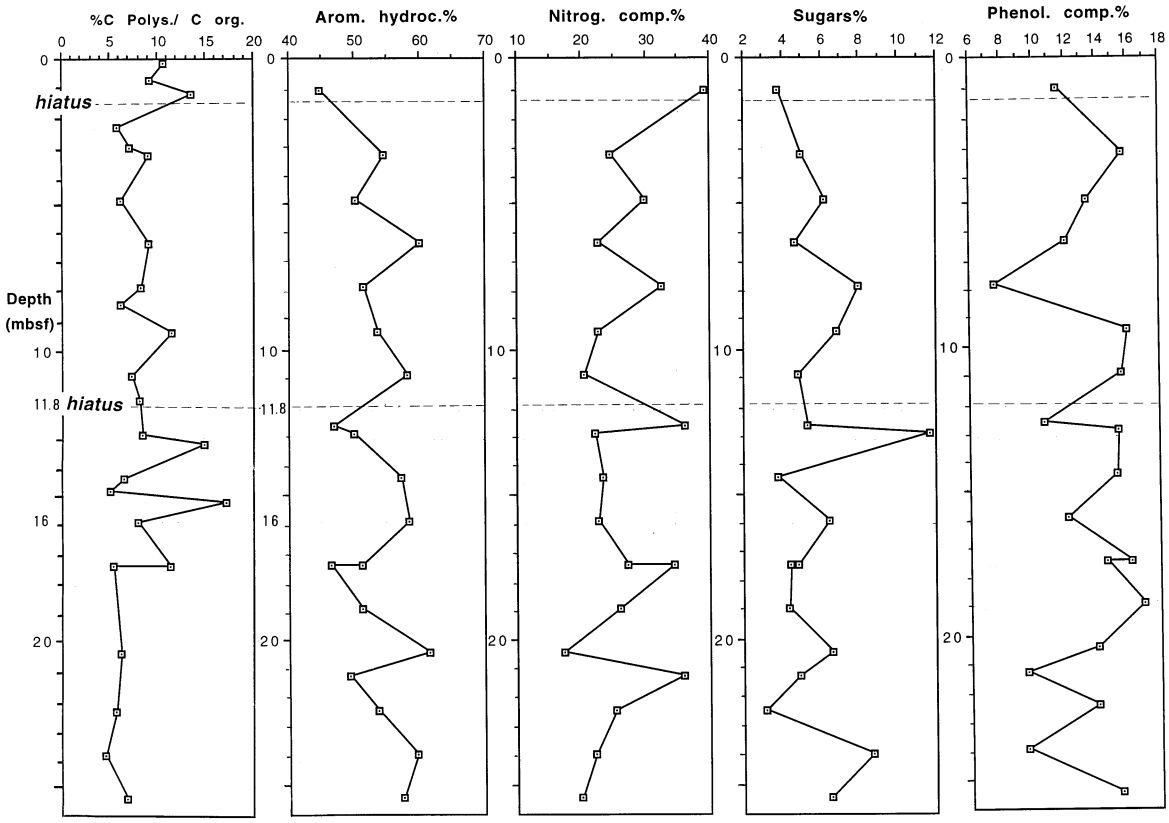

Figure 13. Downhole profiles of polysaccharides (percent in organic carbon) and of the main classes of organic compounds (content percents): aromatic hydrocarbons, nitrogen-containing compounds, sugars, and phenols (PY-GC-MS).

pene structure belong to the cinnamyl series (C). The sum V + S + C represents the real tracer of lignins in sediments, after Hedges and Mann (1979).

Total phenol contents (Fig. 14A), one tracer of terrestrial inputs, greatly increase down to 1 m, (Stage 5). The concentrations are then lower and close to their mean value. An increase is observed from 12.9 to 15.9 mbsf, and from this level contents decrease down to the bottom. They are similar to organic carbon content, which also shows a real increase from 12.9 to 15.9 mbsf (1.58–1.8 Ma) and nearly parallel to the maximum values of polysaccharides (ligno-cellulosic complex?).

In qualitative terms, in the surface layers, the hydroxybenzyl phenols seem to dominate in comparison to the ligneous phenols (syringyls + vanillyls + cinnamyls), according to Hedges and Parker (1976), whereas downward, these ligneous phenols seem to be more resistant and are higher (Fig. 14C). In the less-degraded deposits (the upper meter), an increased supply in organic matter from broad-leaved trees during the onset of the climatic warming of Stage 5 occurred.

The S/V ratio (Hedges and Mann, 1979; Hedges et al., 1988) tends to decrease in the first meter as the polysaccharide contents decrease because the syringyl phenols are more fragile than the vanillyls (Fig. 14C). Three peaks appear at 3.3, 15.9, and 18.9 mbsf and can be interpreted as periods of enhanced supply of as yet undegraded organic matter (Stages 2, 3, and 4 of the last cycle). The occurrence of cinnamyl phenols corresponds to a great extent of grass vegetation (C4 plants). Unfortunately, in general, the contents were lower than the detection limit, and these phenols are apparently missing as a result of their fragility in comparison to syringyls and vanillyls. However, in five levels, C/V ratios (Hedges and Ertel, 1982) close to or higher than 1 were measured: at 0.74 mbsf (Stage 4), C/V = 0.8, corresponding to a pronounced short-term period of aridity with the opening of the rainforest (Maley, 1991), whereas the 14.4- (1.7 Ma) and 15.9-mbsf (1.81 Ma) levels are correlated with the ligneous phenol and polysaccharide episode. Finally, the 23.9- and 25.4-mbsf levels belonging to the very early Pleistocene show C/V values of 0.86 and 1.31, respectively, indicating a grass vegetation (savanna) input. The occurrence of lignin-derived oxidation products is reported here for the first time in sediments dated to at least 2 Ma.

Analysis by PY-GC-MS

Analytical pyrolysis is a useful technique for the characterization of a wide group of complex biological products, insoluble polymers, or compounds adsorbed to a mineral matrix (Wilson et al., 1983). It has also been successfully applied to the characterization of organic matter because it overcomes some of the extraction and solubilization problems of organic matter. It appears to be a suitable technique for studying the characterization of organic matter, especially because of its polymeric nature, which makes analysis by other conventional techniques difficult. PY-GC and PY-GC-MS are degradative analytical techniques in which very few previous treatments are needed and a very small sample amount is required (Granada et al., 1991).

The correlation between pyrolysates and different kinds of original matrices (lignins, carbohydrates, proteins, etc.) is discussed after definition of the main classes of organic compounds: aromatic hydrocarbons, nitrogen-containing compounds, carbohydrates, phenols and amino-sugars (Puigbo et al., 1989).

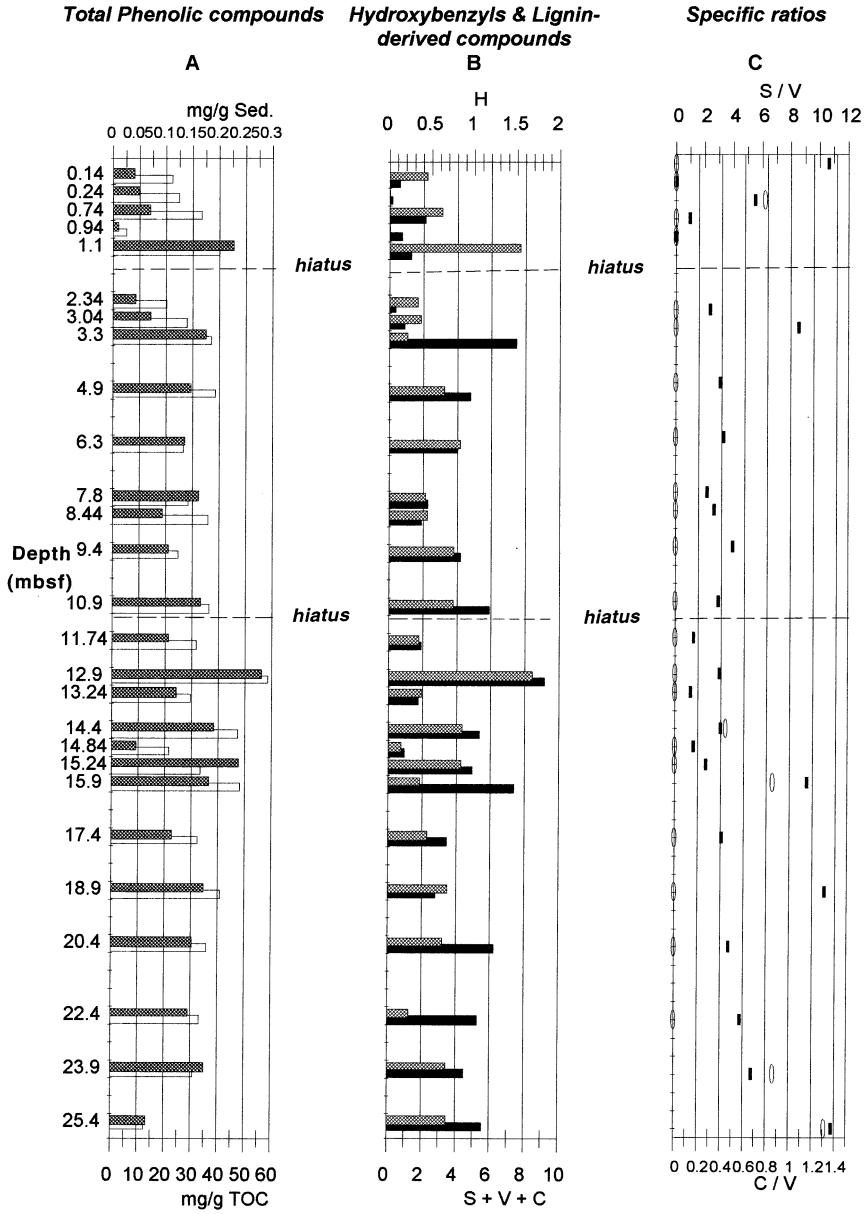

Figure 14. Downhole profiles of phenolic compounds (HPLC analysis). **A.** Phenolic compounds (mg/g dry sediment, open bars) and phenol ‰ in total organic carbon (hatched bars). **B.** Hydroxybenzyls (H, solid bars) and syringyl + vanillyl + cynnamyl (S + V + C, hatched bars) in percent of phenol compounds. **C.** S/V (solid rectangles), and C/V (open ovals) ratios.

Analysis of the four selected main classes of organic compounds (Fig. 13) reveals diverse data:

1. The main character of organic compounds is the high content of aromatic hydrocarbons indicative of adequately degraded organic matter. From the top, the values seem to increase up to 11.9 mbsf, and then the previously observed 13–16 mbsf interval (1.6–1.81 Ma) is individualized. Moreover, the aromatics seem to increase down to the bottom, which shows the influence of diagenesis (degradation and humification). However, the values are irregular, probably related to various increases of marine organic matter or to uneven bottom-current activity.
2. The contents of nitrogen-containing compounds decrease up to the 11.9 mbsf hiatus with an irregular distribution. These components vary inversely to the changes in aromatic contents. The general decrease of these biodegradable compounds with depth is indicative of diagenesis. Their distribution may be also due to their relative increments. They seem lower at the time of the increase of ligneous phenols from 12.9 to 15.9 mbsf and seem higher during the episodes corresponding to the enhanced marine organic matter (Wagner, Chap. 41, this volume)
3. The content of sugars seems to increase up to 13 mbsf. With depth, the values decrease (diagenetic effect).
4. The distribution of phenolic compounds displays several periods of increase (from 2 to 6 m, from 9 to 14 m and from 17 to 20 m). It seems to be somewhat in opposition to that of nitrogen-containing compounds. But these phenolic compounds (pyrolysis fragments) may also be derived from carbohydrates (cyclization) and from proteins (Wilson et al., 1983).

Two characteristic ratios have been analyzed:

1. The furfural + acetic acid/pyrrol ratio (Fig. 15), indicative of the degradation state of organic matter (Bracewell and Robertson, 1984), is higher at 7.5 and 12.9 mbsf, showing a fresher organic material. This ratio is logically opposed to the contents of aromatic carbons, indicative of degraded state. The en-

hanced marine organic matter (Wagner, Chap. 41, this volume) generally corresponds to the higher values of the furfural + acetic acid/pyrrol ratio.

2. The benzene/luene ratio shows many variations (Fig. 15). After a decrease from the surface layers, the lower values from 3.3 to 7.8 meters. Then, they increase from 8.44 to 15.2 m, indicative of more condensed aromatic rings (more degraded organic matter) and then strongly decrease down to the bottom with more constant values. Consequently, the specific character of the 12–15 m interval is once more emphasized.

In terms of individual compounds, constitutive of the above main classes of organic compounds, toluene (aromatic hydrocarbon), a resistant compound, is very low in surface layers and also in the ligneous phenol interval. On the contrary, indol (nitrogenous compound) derived from tryptophane, an unstable amino acid, is very high in surface layers (19%) comparatively to the lower values toward depth (0.6%). Cyclopentenone issued from the aliphatic polycarboxylic acids from soil leaching is increasing at 4.9, from 6.3 to 7.8 and at 14.4 mbsf.

GENERAL COMMENTS AND SUMMARY

The main lithologic characteristics of the Pleistocene deposits at Hole 959C were mainly controlled by a very low sedimentation rate. However, cyclic variations in carbonate, sand fraction, and organic carbon are probably related to a first influence of glacial/interglacial changes. Various patterns were observed: (1) an inverse correlation of organic carbon and bulk carbonate or sands was recorded. Fluctuations, although not strictly connected to glacial/interglacial cycles, are observed in the deposits older than 0.9 Ma and in those younger than 0.12 Ma; (2) the very long gap (0.52 k.y.) between 1.52 and 0.99 Ma is considered the result of the maximum of winnowing caused by enforced bottom currents. This hiatus corresponds to the lower boundary of the section younger than 0.9 Ma, where factors controlling marine sedimentation seem to change significantly; and (3) productivity-driven formation of carbonate-secreting organisms and sand cycles appears enhanced, but inverse correlation with TOC was very contingent. Peaks of organic carbon are observed both during glacial stages (Stages 2, 8, 12, 18, and 20) and interglacial stages (Stages 5, 11, 15, and 25). The increase of carbonate contents after 0.9 Ma may be consistent with an increase in paleoproductivity, but the cyclicity of the deposits was altered by sediment redistribution, causing a frequent mixing of surface and subsurface layers.

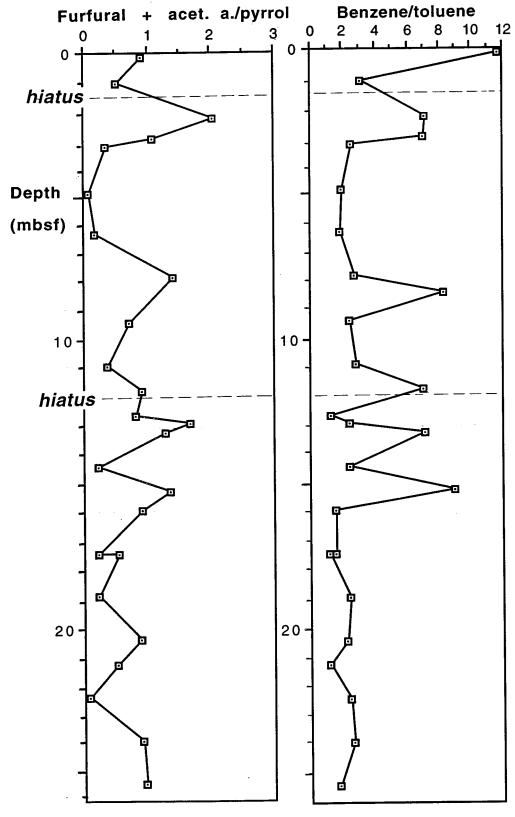

Figure 15. Downhole profiles of furfural + acetic acid/pyrrol ratio and benzene/toluene ratio.

Interference circulation between NADW and SAIW has been drastically enhanced since 1.5 Ma and remained very dynamic during the following time. Consequently, variations in LSR and AR do not appear to be directly related to orbital cycles, but indicate general changes on a much longer time scale.

Between 12 and 11 mbsf, after a long period of reworking, the coarser particles were concentrated. This period of low AR may have resulted in increased neoformation of glauconitic smectite. Uphole, the successive green-grain micro-layers are attributed the same sorting process.

Deductions concerning the adjacent continent's climatic variations could not be obtained directly from the rather uniform Pleistocene clay mineral assemblages. On the other hand, various biogeochemical indicators show the interval 16–13 mbsf to contain a time-transgressive shift of the vegetal landscape; a good agreement exists between the supply of degraded ligneous phenols and the savanna fire markers (J. Maley, pers. comm., 1996). Superimposed on the climatic fluctuation results are several signals of a downhole diagenetic trend: an increase in aromatic hydrocarbons and decreases in polysaccharides, indol, and nitrogen-containing compounds. The grain-size analysis supports evidence for successive bottom-current activities throughout the Pleistocene on this flank rise. Between 2.04 and 1.74 Ma, the episode consisted of enhanced bottom circulation, and between 1.74 and 1.6 Ma, circulation was rather regular and sluggish before persistent enhanced bottom-water velocities resulted in a long, stratigraphic lacuna. After 0.9 Ma, circulation was scattered irregularly, but its main activities seemed concentrated in the upper 3 m, with a second hiatus of 0.08 Ma.

During the late Pleistocene, according to the increased frequency and amplitude of glacio-eustatic oscillations, the lithologic variations were emphasized but partly concealed by the winnowing activity. This period was characterized by repeated lowstand sea levels, with a strong reworking of the emerged Cenozoic deposits of the shelf. Frequently, the occurrence of clinoptilolite and micrite might be correlated with these low sea levels. The parallel increase in eustatic amplitude must correspond during high sea level to a change in the sedimentation regime, but terrigenous supply might have been too distant on a site isolated from gravitational mechanisms.

LONG-TERM PALEOCLIMATIC TRENDS OF THE NEIGHBORING ATLANTIC AREAS

Before the DSDP and ODP investigations, our knowledge of the paleoclimatic events in the eastern equatorial Atlantic had been restricted to the Kane fracture zone between 3° and 8° N (Ruddiman, 1971). Deep-sea cores were collected between 3100 and 5200 m water depth and carbonate removal by dissolution on the seafloor was evaluated, along with terrigenous lutite dilution and carbonate productivity variation. Two main episodes were found: (1) at 1.3 Ma, the climatic situation deteriorated, and short but severe cold pushes began to break off the previous warmth record of the late Matuyama;

and (2) after 0.9 Ma, the duration of cold episodes increased and the terrigenous dilution depressed the percentage of carbonate (Fig. 16). This change in range might be correlated with the Hole 959C change, where we observed that 1.3 Ma corresponds to the middle age of the major lacuna, and 0.9 Ma, always with winnowing activity, might present a higher amplitude of carbonate and sand fraction-curve oscillations.

On the northwest African margin (Sarnthein et al., 1982), planktonic and benthic foraminifer counts and oxygen-isotopic records suggest important interaction between upwelling and eolomarine dust inputs, particularly during the glacial modes. So each interval cannot be correlated with the one of Hole 959C, where the signal is partly distorted, but the stepwise general climatic trend presents from 1.9 to 0.73 Ma an early standstill of deterioration where coastal upwelling reached its absolute maximum, then a second-step deterioration was recorded after 0.7 Ma, where all sedimentary parameters began to vary with increased amplitudes. At the same time, fertility of coastal upwelling retreated and the bulk sediment accumulation decreased (although eolian dust increased). Various characteristics of paleoenvironments (planktonic foraminifer assemblages and terrigenous discharge) indicate that the main changes occurred somewhat earlier, near 0.9 Ma, as a result of a drop in equatorial sea-surface temperature (Fig. 16). If all these changes show that the ocean and land did not respond in a synchronous way to global events, the beginning change near 0.9 Ma seems to be a slightly delayed onset of the Guinea Gulf events.

Few records from the Southern Hemisphere present long-term trends. However, some evidence favors the possibility of linkage with the equatorial trends. On the Walvis Ridge beneath the Benguela Current, opal fluxes decreased during the Brunhes Chron (Dean et al., 1984), namely, after 0.73 Ma. In the Congo-Zaire deep-sea fan, Jansen et al. (1986) described episodes of lower sedimentation rate of terrigenous sediment during the last 0.35 m.y. as a shift toward a more humid (warmer) climate in south equatorial Africa.

The changes in the last 2.4 m.y. recorded off Africa during Leg 108 from the equator to about 20°N were synthesized by Ruddiman et al. (1989) and deMenocal et al. (1993). This overview is the most accurate reference on this work (Fig. 16). With some differences connected to the latitude, surface waters from as far as north as the equatorial Atlantic to as far as south as the subantarctic may have reached an extreme cooling state late in the Pliocene or early in the Pleistocene. Off Mauritania, the decrease in accumulation rate of terrigenous sediment fraction between 3.1 and 2.45 ka indicates the change from a predominantly humid climate to a climate of arid/humid cycles typical of the last 2.45 m.y. (Stein et al., 1989). It is interesting to note that the first major glacial event off Mauritania predates the one formed near the Equator by about 300 k.y. (Sarnthein and Tiedemann, 1989). Two changes that are concentrated along the northwestern margin of the Sahara are the abrupt increase in fluxes of both opal and winter plumes dust. This timing cannot indicate a direct connection to the delayed onset of ice sheets in the Northern Hemisphere. It appears to be linked to the continued cooling of the Antarctic region.

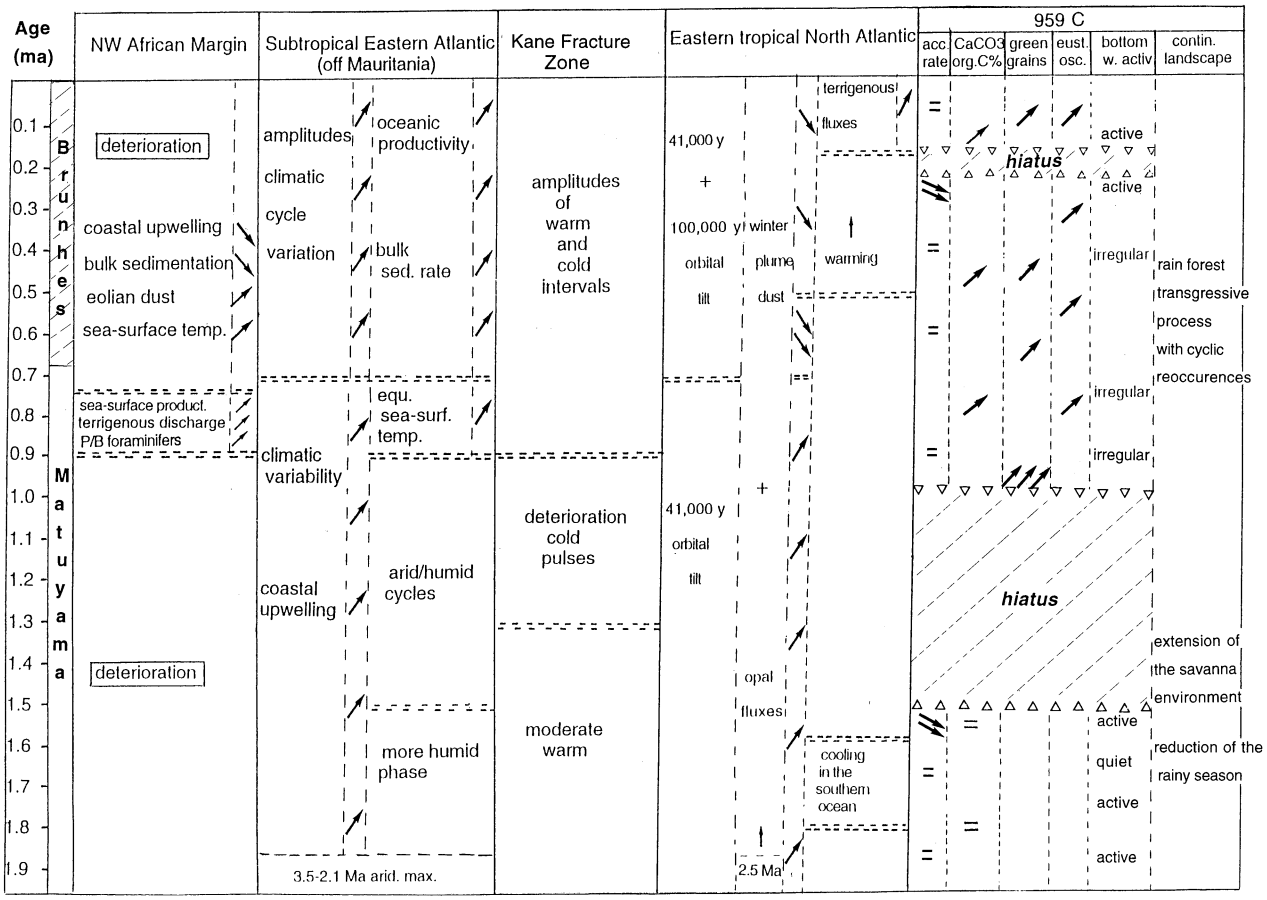

Figure 16. Schematic diagram of several Pleistocene records from the Atlantic margin of Africa based on Ruddiman (1971), Ruddiman et al. (1989), Sarnthein et al. (1982), Stein et al. (1989), and Tiedemann et al. (1989); comparison with Site 959 record as a whole.

Near the modern antarctic convergence, sedimentary records present a shift from calcareous to siliceous deposition near 1.6 Ma (at the beginning of the Hole 959C hiatus). This shift may be representative of a major cooling and/or restructuring of circumantarctic circulation. Effects of the tectonic uplift of the Tibetan Plateau caused drying along the northwest African margin and wetter conditions in the tropics and western Sahel (Ruddiman et al., 1989). In the Guinea Gulf, this tropicalization results from an increased rising motion and monsoonal inflow. This opposite change should have had some effects on the apparent diachronism of the eastern equatorial Atlantic.

During the last 0.7 m.y., the amplitude variation of the climatic cycles distinctly increased. The ice-volume fluctuations at the 41-k.y. period of orbital till yielded to the larger 100-k.y. fluctuations (Shackleton and Opdyke, 1976). This resulted in a stronger decrease in dust and opal fluxes (but an increase in percentages) than equatorial sites. During this period, fluxes along the Mauritanian margin are probably controlled by factors different from along the equator. Ruddiman and Janecek (1989) suggested that the strong zonal flow of southern trade winds exerted a decisive influence upon the equator from 2.4 to 0.7 Ma. Then, these winds reverted back to more meridional flow during boreal summers, which would have led to a suppressed opal deposition caused by weaker zonal winds.

COMPARISON TO HOLE 959C AND CONCLUSIONS

The vertical distribution of the paleoenvironmental indicators recorded in the Pleistocene of Hole 959C, in spite of superimposed winnowing activities and a consequent hiatus, could be correlated with the major modifications observed in the sedimentation regime of the nearby Atlantic areas. But it shows different and specific features that correspond to geographic or topographic factor controls.

The slow AR observed during the early Pleistocene accounts for the more significant event of the record. The brief maximum of this process from 1.52 to 0.99 Ma resulted in a major stratigraphic lacuna. Based on the green grain concentration, the first deposits of the new beginning of sedimentation clearly show repetitive reworking. Winnowing exceeded detrital influx, producing accumulation rates that prevent glauconite formation.

At Site 959, located near the southern boundary of wind-blown detritus, very few eolian dusts were likely to reach the oceanic bottom. According to the vertical distribution of the relative abundance of quartz in the total sample, this presumed flux seems rather uniform. However, amplitudes of fluctuation increase during the last 0.7 m.y. and some peaks are related to glacial episodes. No significant change seems to have been reported in mineralogical composition. The clay mineral assemblages were composed of the same major minerals (kaolinite, smectite, and illite) throughout the Pleistocene deposits. Only illite contents indicate the increase of the last 0.9 Ma glacio-eustatic event and especially the reworking of the emerged shelf. Whatever climatic oscillations might have occurred on land, the geochemical budget of the soils did not significantly vary. In return, the lignine phenols document a noticeable aridification and, consequently, an opening of the rainforest (precisely between 1.8 and 1.5 Ma) on the African continent. This landscape shift is consistent with the strongest eolian supply of grass plant debris to the northern Gulf of Guinea (Wagner, Chap. 41, this volume). Another maybe more significant control factor may be the elevated location of Site 959 on the eastern flank of the rise and its relative isolation from the direct gravity-induced transport. Only a small part of the slope-borne material was able to reach the plateau of the flank. The consequence of this isolation would be enhanced during the late Pleistocene, just after the increase of the glacio-eustatic oscillations: the higher frequency of highstand sea level suggests a possible weakening supply control by the removal of the shoreline. The early Pleistocene showed a large sea-level drop in conjunction with the first occurrence of extensive glaciations on the Northern Hemisphere (Vail et al., 1977).

After 0.9 Ma, the magnitude of coupled climatic and eustatic oscillations strongly increased. If we consider a relatively constant accumulation rate, the amplitude variation of the carbonate fluxes may have reached 25% in spite of micrite reworking interference during lowered sea level. The carbonate signal of these oscillations is recorded all the more as there are few interferences with other processes like sedimentation rate increase, upwelling influence, wind-blown dusts, or downslope sediment fluxes, as was reported from adjacent basins in the eastern subtropical Atlantic. It is also suggested that the apparent early character of these high-amplitude variations was promoted by such specific conditions. Despite the diachronism, we observe similar effects to the major decrease in opal and terrigenous fluxes over the last 0.7–0.5 m.y. at equatorial Sites 663 and 664, the less distant sites of Leg 108, or also of the increase in cold episodes after 0.9 Ma in the Kane fracture zone (Ruddiman, 1971; Ruddiman et al., 1989).

In short, and with some apparent chronological shiftings or some local effects mainly connected with the topographic situation, the results of this lithologic and geochemical study from Site 959 of Leg 159 correlate with those of the previous Leg 108. They support one of the assumptions of the more immediate control of the equatorial ocean by the sub-Antarctic Ocean (Ruddiman and Janecek, 1989), possibly accompanied by increased forcing of northward flowing AAIW. Here, such change in circulation played an important role in increasing the amount of circulation and was responsible for the long stratigraphic lacunae.

ACKNOWLEDGMENTS

We thank Patrick Barthe, Jean-Louis Blazy, and Jose Luis Liberia for laboratory work and their helpful assistance in general, and the Shipboard Scientific Party of Leg 159 for providing us with samples from Hole 959C (especially the assistance of Tom Wagner and Jean Benkhelil). We are indebted to Institut Quimic de Sarria (Barcelona) for the use of their PY-GC-MS technique. We gratefully thank Dr. T. Wagner and one anonymous reviewer for the improvement of the manuscript. Support by ODP-France and INSU-CNRS is greatly appreciated. This is a URA 715 CNRS and LEA Sciences de la Mer contribution.

REFERENCES

Berger, W.H., and Winterer, E.L., 1974. Plate stratigraphy and the fluctuating carbonate line. *In* Hsü, K.J., and Jenkyns, H.C. (Eds.), *Pelagic Sediments on Land and Under the Sea.* Spec. Publ. Int. Assoc. Sedimentol., 1:11–48.

Biscaye, P.E., 1965. Mineralogy and sedimentation of recent deep-sea clays in the Atlantic Ocean and adjacent seas and oceans. *Geol. Soc. Am. Bull.*, 76:803–832.

Blarez, E., 1986. La marge continentale de Côte d'Ivoire-Ghana: structure et évolution d'une marge continentale transformante [Ph.D. thesis]. Univ. Pierre et Marie Curie, Paris.

Bonifay, D., and Giresse, P., 1992. Middle to late Quaternary sediment flux and post-depositional processes between the continental slope off Gabon and the Mid-Guinean margin. *Mar. Geol.*, 106:107–129.

Bowles, F.A., 1975. Paleoclimatic significance of quartz/illite variations in cores from the Eastern Equatorial North-Atlantic. *Quat. Res.*, 5:225–235.

Bracewell, J.M., and Robertson, G.W., 1984. Characteristics of soil organic matter in temperate soils by Curie point pyrolysis-mass spectrometry. I: Organic matter variations with drainage and mull humification in A horizons. *J. Soil Sci.*, 35:549–558.

Chamley, H., 1980. Clay sedimentation and paleoenvironment in the area of Daito Ridge (Northwest Philippine Sea) since the early Eocene. *In* Klein,

G. de V., Kobayashi, K., et al., *Init. Repts. DSDP,* 58: Washington (U.S. Govt. Printing Office), 683–693.

Chen, C.L., and Chang, H.M., 1989. Chemistry of lignin biodegradation. *In* Higuchi T. (Ed.), *Biosynthesis and Biodegradation of Wood Components* (Vol. 19): Orlando (Academic Press), 535–556.

Creighton, R.H.J., Gibbs, R.D., and Hibbert, H., 1944. Studies on lignin and related compounds. LXXV. Alkaline nitrobenzene oxidation of plant materials and application to taxonomic classification. *J. Chem. Soc*., 66:32–37.

Creighton, R.H.J., and Hibbert, H., 1944. Studies on lignins and related compounds. LXXVI. Alkaline nitrobenzene oxidation of corn stalks: isolation of p-hydroxybenzaldehyde. *J. Chem. Soc*., 66:37–40.

Damuth, J.E., 1975. Quaternary climate change as revealed by calcium carbonate fluctuations in western equatorial Atlantic sediments. *Deep-Sea Res. Part A,* 22:725–743.

Dean, W.E, Hay, W.W., and Sibuet, J.-C., 1984. Geologic evolution, sedimentation, and paleoenvironment of the Angola Basin and adjacent Walvis Ridge, synthesis of results of Deep-Sea Drilling Project Leg 75. *In* Hay, W.W., Sibuet, J.-C., et al., *Init. Repts. DSDP,* 75 (Pt. 1): Washington (U.S. Govt. Printing Office), 509–544.

deMenocal, P.B., Ruddiman, W.F., and Pokras, E.M., 1993. Influence of high- and low-latitude on African terrestrial climate: Pleistocene eolian records from equatorial Atlantic Ocean Drilling Program Site 663. *Paleoceanography,* 8:209–242.

Farmer, V.C., and Morrison, R.I., 1964. Lignin in Sphagnum and Phragmites and in peats derived from these plants. *Geochim. Cosmochim. Acta,* 28:1537–1546.

Faugères, J.C., Legigan, P., Maillet, N., Sarnthein, M., and Stein, R., 1989. Characteristics and distribution of Neogene turbidites at Site 657 (Leg 108, Cap Blanc continental rise, Northwest Africa): variations in turbidite source and continental climate. *In* Ruddiman, W., Sarnthein, M., et al., *Proc. ODP, Sci. Results*, 108: College Station, TX (Ocean Drilling Program), 329–348.

Freudenberg, K., and Neish, A.C., 1968. *Constitution and Biosynthesis of Lignin.* Berlin (Springer-Verlag).

Gallali, T., 1972. Etude statique et dynamique des polysaccharides et des aminopolysaccharides au cours de l'humification [thesis]. Nancy Univ.

Giresse, P., and Odin, G.S., 1973. Nature minéralogique et origine des glauconies du plateau continental du Gabon et du Congo. *Sedimentology,* 20:457–488.

Granada, E., Blasco, J., Comellas, L., and Gassiot, M., 1991. Pyrolysis-gas chromatography analyses of organic matter in soils using nitrogen-selective detection. *J. Anal. Appl. Pyrolysis*, 19:193–202.

Griffin, J.J., Windom, H., and Goldberg, E.D., 1968. The distribution of clay minerals in the World Ocean. *Deep-Sea Res. Part A,* 15:433–459.

Harborne, J.B., 1964. *Biochemistry of Phenolic Compounds:* London (Academic Press).

————, 1980. Plant phenolics. *In* Bell, E.A., and Charlwood, B.V. (Eds), *Secondary Plant Products:* Berlin (Springer-Verlag), 310–402.

Hartley, R.D., and Buchan, H., 1979. High-performance liquid chromatography of phenolic acids and aldehydes derived from plants or from the decomposition of organic matter in soil. *J. Chromatogr.,* 180:139–143.

Hays, J.D., Imbrie, J., and Shackleton, N.J., 1976. Variations in the Earth's orbit: pacemaker of the ice ages. *Science,* 194:1121–1132.

Hedges, J.I., Clark, W.A., and Cowie, G.L., 1988. Organic matter sources to the water column and surficial sediments of a marine bay. *Limnol. Oceanogr.,* 33:1116–1136.

Hedges, J.I., and Ertel, J.R., 1982. Characterization of lignin by capillary gas chromatography of cupric oxide oxidation products. *Anal. Chem*., 54:174–178.

Hedges, J.I., and Mann, D.C., 1979. The lignin geochemistry of marine sediments from the southern Washington coast. *Geochim. Cosmochim. Acta,* 43:1809–1818.

Hedges, J.I., and Parker, P.L., 1976. Land derived organic matter in surface sediments from the Gulf of Mexico. *Geochim. Cosmochim. Acta,* 40:1019–1029.

Jacobi, R., and Hayes, D., 1982. Bathymetry, microphysiography and reflectivity characteristics of the West African margin, between Sierra Leone and Mauritania. *In* von Rad, O., Hinz, K., Sarnthein, M., and Seibold, E. (Eds), *Geology of the Northwest African Continental Margin:* Berlin (Springer-Verlag), 182–212.

Jansen, J.H.F., Kuijpers, A., and Troelstra, S.R., 1986. A mid-Brunhes climatic event: long-term changes in global atmospheric and ocean circulation. *Science,* 232:619–622.

Jansen, J.H.F., and van der Gaast, S.J., 1988. Accumulation and dissolution of opal in Quaternary sediments of the Zaire deep-sea fan (northeastern Angola Basin). *Mar. Geol.,* 83:1–7.

Jansen, J.H.F., van Weering, T.G.E., Gieles, R., and van Iperen, J., 1984. Middle and late Quaternary oceanography and climatology of the Zaire-Congo fan and the adjacent eastern Angola Basin. *Neth. J. Sea Res.,* 17:201–241.

Johnson, D.A., 1985. Abyssal teleconnections II. Initiation of Antarctic Bottom Water flow in the southwest Atlantic. *In* Hsü, K.J., and Weissert, H.J. (Eds.), *South Atlantic Paleoceanography:* Cambridge (Cambridge Univ. Press), 243–281.

Kounkou, G.L., and Barusseau, J.P., 1988. Terrigenous sedimentation of the upper Quaternary in the Cayar deep-sea fan (Senegal-Gambia abyssal plain-Atlantic ocean). *Oceanol. Acta,* 11:359–368.

Lewis, N.G., and Yamamoto, E., 1990. Lignin: occurrence, biogenesis, and biodegradation. *Annual Rev.—Plant Physiol. Plant Mol. Biol.,* 41:455–496.

Maley, J., 1991. The African rain forest vegetation and palaeoenvironment during late Quaternary. *Clim. Change,* 19:79–98.

McIntyre, A., Ruddiman, W.F., Karlin, K., and Mix, A.C., 1989. Surface water response of the equatorial Atlantic Ocean to orbital forcing. *Paleoceanography,* 4:19–55.

Morley, J.J., 1977. Upper Pleistocene climatic variations in the South-Atlantic derived from a quantitative Radiolarian analysis: accent on the last 18,000 years [thesis]. Columbia Univ., New York.

Morley, J.J., and Hays, J.D., 1981. Towards a high-resolution, global, deep-sea chronology for the last 750,000 years. *Earth Planet. Sci. Lett.,* 53:279–295.

Odin, G.S., and Fullagar, P.D., 1988. Geological significance of the glaucony facies. *In* Odin, G.S. (Ed.), *Green Marine Clays:* Amsterdam (Elsevier), Dev. in Sedimentol. Ser., 45:295–332.

Odin, G.S., and Matter, A., 1981. Die glauconarium origine. *Sedimentology,* 28:611–643.

Pearl, I.A., 1942. Vanillin from lignin materials. *J. Am. Chem. Soc.,* 64:1429–1431.

Pokras, E.M., and Molfino, B., 1986. Oceanographic control of diatom abundances and species distributions in surface sediments of the tropical and southeast Atlantic. *Mar. Micropaleontol.,* 10:165–188.

Puigbo, A., Gadel, F., Alcaniz, J.M., and Comellas, L., 1989. PY-GC-MS analysis of organic matter in suspended material and deposits of the submarine delta of the Rhone river (France). *Sci. Total Environ.,* 81–82:71–80.

Riviere, A., 1977. *Méthodes Granulometrics: Techniques et Interpretations:* Paris (Masson).

Robert, C., 1982. Modalité de la sédimentation argileuse en relation avec l'histoire géologique de l'Atlantique Sud [Ph.D. dissert.]. Univ. Aix-Marseille, France.

Ruddiman, W.F., 1971. Pleistocene sedimentation in the equatorial Atlantic: stratigraphy and faunal paleoclimatology. *Geol. Soc. Am. Bull.,* 82:283–302.

Ruddiman, W.F., and Janecek, T.R., 1989. Pliocene-Pleistocene biogenic and terrigenous fluxes at equatorial Atlantic Sites 662, 663, and 664. *In* Ruddiman, W., Sarnthein, M., et al., *Proc. ODP, Sci. Results,* 108: College Station, TX (Ocean Drilling Program), 211–240.

Ruddiman, W.F., Sarnthein, M., Backman, J., Baldauf, J.G., Curry, W., Dupont, L.M., Janecek, T., Pokras, E.M., Raymo, M.E., Stabell, B., Stein, R., and Tiedemann, R., 1989. Late Miocene to Pleistocene evolution of climate in Africa and the low-latitude Atlantic: overview of Leg 108 results. *In* Ruddiman, W., Sarnthein, M., et al., *Proc. ODP, Sci. Results,* 108: College Station, TX (Ocean Drilling Program), 463–484.

Sarkanen, K.V., and Hergert, H.L., 1971. Lignins in the plant kingdom: classification and distribution. *In* Sarkanen, K.V., and Ludwig, C.H. (Eds), *Lignins: Occurrence, Formation Structure and Reaction* (Pt. 2): New York (Wiley-Interscience), 43–94.

Sarnthein, M., Tetzlaff, G., Koopmann, B., Wolter, K., and Pflaumann, U., 1981. Glacial and interglacial wind regimes over the eastern subtropical Atlantic and Northwest Africa. *Nature,* 293:193–196.

Sarnthein, M., Thiede, J., Pflaumann, U., Erlenkeuser, H., Fütterer, D., Koopmann, B., Lange, H., and Seibold, E., 1982. Atmospheric and oceanic circulation patterns off Northwest Africa during the past 25 million years. *In* von Rad, U., Hinz, K., Sarnthein, M., Seibold, E. (Eds.), *Geology of the Northwest African Continental Margin:* Berlin (Springer Verlag), 545–604.

Sarnthein, M., and Tiedemann, R., 1989. Toward a high-resolution stable isotope stratigraphy of the last 3.4 million years: Sites 658 and 659 off

northwest Africa. *In* Ruddiman, W., Sarnthein, M., et al., *Proc. ODP, Sci. Results,* 108: College Station, TX (Ocean Drilling Program), 167–185.

Scribe, P., and Bourdier, G., 1995. La matiere organique la custre: affroche par les marqueurs moleculairs. *In* Pourriot, R. and Meybeck, M. (Eds.), *Limnologie générale. Collection d'Ecologie,* 25: Paris (Masson), 157–186.

Serve, L., and Piovetti, L., 1984. Dosage par chromatographie liquide haute performance des composés phénoliques libres par hydrolyse dacides humiques. *J. Chromatogr.*, 292:458–467.

Serve, L., Piovetti, L., and Longuemard, N., 1983. Dosage des acides et aldéhydes phénoliques par chromatographie liquide haute performance: analyse comparative des sols de haute montagne et de leur végétation. *J. Chromatogr.*, 259:319–338.

Shackleton, N.J., and Opdyke, N.D., 1976. Oxygen-isotope and paleomagnetic stratigraphy of Pacific Core V28-239: late Pliocene to latest Pleistocene. *In* Cline, R.M., and Hays, J.D. (Eds.), *Investigations of Late Quaternary Paleoceanography and Paleoclimatology.* Mem.—Geol. Soc. Am., 145:449–464.

Shipboard Scientific Party, 1996. Site 959. *In* Mascle, J., Lohmann, G.P., Clift, P.D., et al., *Proc. ODP, Init. Repts.*, 159: College Station, TX (Ocean Drilling Program), 65–150.

Siegel, P., 1969. Evidence for the presence of lignin in most gametophytes. *Am. J. Bot.*, 56:175–179.

Stabell, B., 1989. Initial diatom record of Sites 657 and 658: on the history of upwelling and continental aridity. *In* Ruddiman, W., Sarnthein, M., et al., *Proc. ODP, Sci. Results*, 108: College Station, TX (Ocean Drilling Program), 149–156.

Stein, R., and Faugères, J.-C., 1989. Sedimentological and geochemical characteristics of the Upper Cretaceous and lower Tertiary sediments at Site 661 (eastern equatorial Atlantic) and their paleoenvironmental significance. *In* Ruddiman, W., Sarnthein, M., et al., *Proc. ODP, Sci. Results*, 108: College Station, TX (Ocean Drilling Program), 297–309.

Stein, R., ten Haven, H.L., Littke, R., Rullkötter, J., and Welte, D.H., 1989. Accumulation of marine and terrigenous organic carbon at upwelling Site 658 and nonupwelling Sites 657 and 659: implications for the reconstruction of paleoenvironments in the eastern subtropical Atlantic through late Cenozoic times. *In* Ruddiman, W., Sarnthein, M., et al., *Proc. ODP, Sci. Results*, 108: College Station, TX (Ocean Drilling Program), 361–385.

Tiedemann, R., Sarnthein, M., and Stein, R., 1989. Climatic changes in the western Sahara: aeolo-marine sediment record of the last 8 million years (Sites 657–661). *In* Ruddiman, W., Sarnthein, M., et al., *Proc. ODP, Sci. Results*, 108: College Station, TX (Ocean Drilling Program), 241–277.

Towers, G.H.N., and Gibbs, R.D., 1953. Lignin chemistry and the taxonomy of higher plants. *Nature*, 172:25–26.

Vail, P.R., Mitchum, R.M., Jr., and Thompson, S., III, 1977. Seismic stratigraphy and global changes of sea level, Part 2. The depositional sequence as a basic unit for stratigraphic analysis. *In* Payton, C.E. (Ed.), *Seismic Stratigraphy: Applications to Hydrocarbon Exploration.* AAPG Mem., 26:53–62.

Van Bennekom, A.J., and Berger, G.W., 1984. Hydrography and silica budget of the Angola Basin. *Neth. J. Sea Res.*, 17:149–200.

Verardo, C.D.J., and McIntyre, A., 1994. Production and destruction: control of biogenous sedimentation in the tropical Atlantic 0–300,000 years B.P. *Paleoceanography,* 9:63–86.

Verstraete, J.-M., 1992. The seasonal upwellings in the Gulf of Guinea. *Progr. Oceanogr.*, 29:1–60.

Voituriez, B., and Herbland, A., 1982. Comparaison des systèmes productifs de l'Atlantique tropical Est: dômes thermiques, upwelling côtier et upwelling équatorial. *Rapp. P.-V., Reun. Cons. Int. Explor. Mer,* 180:114–130.

Wilson, M.A., Philip, R.P., Gillam, A.H., and Tate, K.R., 1983. Comparison of the structures of humic substances from aquatic and terrestrial sources by pyrolysis-gas chromatography-mass spectrometry. *Geochim. Cosmochim Acta,* 47:497–502.

Date of initial receipt: 17 September 1996
Date of acceptance: 1 April 1997
Ms 159SR-041